

*D. Matthews*

**SATELLITE STUDIES  
DURING THE 1976-77 , 1977- 78  
SIERRA COOPERATIVE PILOT  
PROJECT**

**By**

**K. ROBERT MORRIS  
DAVID W. REYNOLDS  
THOMAS H VONDER HAAR**



**FINAL REPORT  
BUREAU OF RECLAMATION  
CONTRACT #6-07-DR-20020  
FEBRUARY, 1979**

**DEPARTMENT OF ATMOSPHERIC SCIENCE  
COLORADO STATE UNIVERSITY  
FORT COLLINS, COLORADO**

SATELLITE STUDIES DURING THE 1976-77  
1977-78 SIERRA COOPERATIVE PILOT PROJECT

by

K. Robert Morris  
David W. Reynolds  
Thomas H. Vonder Haar

Department of Atmospheric Science  
Colorado State University

Final Report to the  
Office Atmospheric Resources Management  
Bureau of Reclamation, Denver, Colorado 80225  
Under Contract 6-07-DR-20020

Technical Monitor: David A. Matthews, Bureau of Reclamation  
Denver, Colorado 80225

February 1979

## ABSTRACT

### SATELLITE STUDIES DURING THE 1976-77 AND 1977-78 SIERRA COOPERATIVE PILOT PROGRAM

Digital imagery from the SMS-2 geostationary satellite was recorded for analysis in support of the Sierra Cooperative Pilot Project.

Imagery of five storms during the 1976-77 and 1977-78 seasons of the project have been analyzed in detail using the CSU ADVISAR. Temporal variations in cloud top temperature were charted and synoptic and meso-scale cloud features have been studied.

Results show the highest precipitation and lowest cloud top temperatures, below  $-35^{\circ}\text{C}$ , occur about one or two hours ahead of the surface cold front within the frontal band. Following the frontal passage, an unstable convective orographic cloud remains over the Sierra for up to 8 hours, with cloud top temperatures around  $-15^{\circ}\text{C}$ , well within the seeding window range.

Mesoscale features including banded and cellular convection and cloud streets have been observed by the satellite, with their effects often showing up in the precipitation gage records. Large convective lines and cells were tracked onshore and were found to move with the winds somewhat below the 50 kPa level. Cells intensify in the Central Valley of California, usually dissipating as they climb the Sierra. Trajectories of large cells curve to the left upon encountering the foothills, becoming nearly parallel to the mountains under certain conditions.

Precipitation is greatest on the west slopes of the Sierra due to the orographic effect. Lee-side precipitation appears to be dependent on the presence of high, cold cloud tops which lead to precipitation particles being carried over the crest.

TABLE OF CONTENTS

	Page
ABSTRACT. . . . .	i
TABLE OF CONTENTS . . . . .	ii
LIST OF FIGURES . . . . .	iii
1.0 INTRODUCTION. . . . .	1
A. Background. . . . .	1
B. Scientific Objectives . . . . .	1
2.0 SATELLITE OBSERVATION AND TECHNIQUES. . . . .	4
A. Geostationary Satellite Data for the Sierra Project . . . . .	4
B. Navigating the Satellite Imagery. . . . .	5
C. Digital Image Display and Processing. . . . .	6
I. The CSU ADVISAR . . . . .	6
II. ADVISAR Capabilities. . . . .	6
III. Color Enhancement of Digital Imagery. . . . .	8
3.0 CLOUD CHARACTERISTICS OF SIERRA STORMS. . . . .	9
A. Convective Cells and Bands. . . . .	9
B. Sierra Orographic Clouds. . . . .	11
4.0 INTENSIVE CASE STUDIES	
4.1 9 MARCH 1977 CASE STUDY . . . . .	13
4.2 14-15 DECEMBER 1977 CASE STUDY. . . . .	19
4.3 17-18 DECEMBER 1977 CASE STUDY. . . . .	27
4.4 8-9 FEBRUARY 1978 CASE STUDY. . . . .	32
4.5 2-3-4 MARCH 1978 CASE STUDY . . . . .	40
A. General Description . . . . .	40
B. 2 March 1978. . . . .	41
C. 3 March 1978. . . . .	53
D. 4 March 1978. . . . .	61
E. Summary of the 2-3-4 March 1978 Storm . . . . .	70
5.0 CONCLUSIONS . . . . .	74
6.0 RECOMMENDATIONS FOR FUTURE WORK . . . . .	86
ACKNOWLEDGEMENTS. . . . .	37
REFERENCES. . . . .	88

## LIST OF FIGURES

Figure		Page
1	Map of SSCP project Area. . . . .	2
2	Satellite-observed CTT, 9 March 1977. . . . .	14
3	Raingage records for Plavada and Auburn, 9 March 1977 .	15
4	Raingage records for Blue Canyon and Donner Summit, 9 March 1977. . . . .	16
5	1715 GMT, 9 March 1977 visible image. . . . .	18
6	Composite 70 and 50 kPa observations, 1200 GMT, 15 December 1977 . . . . .	20
7	Satellite-observed CTT, 14-15 December 1977 . . . . .	22
8	Raingage records for Blue Canyon and Donner Summit, 14-15 December 1977 . . . . .	23
9	0445 GMT, 15 December 1977 IR image . . . . .	25
10	Satellite-observed CTT, 17-18 December 1977 . . . . .	28
11	Raingage records for Blue Canyon, Donner Summit and Truckee, 17-18 December 1977. . . . .	29
12	1945 GMT, 17 December 1977 visible image. . . . .	30
13	2045 GMT, 17 December 1977 IR image . . . . .	25
14	2245 GMT, 8 February 1978 visible image . . . . .	33
15	Satellite-observed CTT, 8-9 February 1978 . . . . .	34
16	Raingage records for Blue Canyon, Donner Summit and Truckee, 8-9 February 1978. . . . .	35
17	0915 GMT, 9 February 1978 IR image. . . . .	25
18	Surface analysis for 1200 GMT, 9 February 1978. . . . .	38
19	1215 GMT, 9 February 1978 IR image. . . . .	25
20	2045 GMT, 9 February 1978 visible image . . . . .	39
21	Satellite-observed CTT, 2-3 March 1978. . . . .	42

Figure		Page
22	1915 GMT, 2 March 1978 visible image. . . . .	43
23	50 kPa analysis for 1200 GMT, 2 March 1978. . . . .	44
24	2045 GMT, 2 March 1978 visible image. . . . .	43
25	2045 and 2145 GMT, 2 March 1978 IR images . . . . .	49
26	Raingage records for Blue Canyon, Donner Summit and Truckee, 2-3 March 1978 . . . . .	50
27	Surface analysis for 2100 GMT, 2 March 1978 . . . . .	51
28	Raingage record for Sheridan, 2-3 March 1978. . . . .	54
29	2215 GMT, 3 March 1978 visible image. . . . .	57
30	2015 GMT, 3 March 1978 visible image. . . . .	57
31	Satellite-observed CTT, 3-4 March 1978. . . . .	59
32	2345 GMT, 3 March 1978 visible image. . . . .	60
33	Raingage records for Blue Canyon, Donner Summit and Truckee, 3-4 March 1978 . . . . .	62
34	Raingage record for Sheridan, 3-4 March 1978. . . . .	63
35	1345 GMT, 4 March 1978 IR image . . . . .	49
36	Surface analysis for 1500 GMT, 4 March 1978 . . . . .	66
37	1745 GMT, 4 March 1978 visible image. . . . .	67
38	Cloud photo from aircraft at 1830 GMT, 4 March 1978. . . . .	67
39	1845 GMT, 4 March 1978 IR image . . . . .	49
40	1915 GMT, 4 March 1978 visible image. . . . .	69
41	Cloud photo from aircraft at 1857 GMT, 4 March 1978. . . . .	69
42	Three storm averages of mean target area CTT relative to time from frontal passage . . . . .	82
43	Six storm mean hourly precipitation at Blue Canyon relative to time from frontal passage . . . . .	84

## 1. INTRODUCTION

### A. Background

During the winter seasons of 1976-77 and 1977-78, CSU (under Contract 6-07-DR-20020) collected digital imagery from the SMS-2 geostationary satellite for analysis in support of the Sierra Cooperative Pilot Project (SCPP) being conducted by the U.S. Bureau of Reclamation. The intent of this project was to study in detail the application of digital geosynchronous satellite imagery to the SCPP. An earlier report (Reynolds, 1977) contained preliminary results for the 1976-77 field program. This current report includes final results for the 1976-77 period plus results from the 1977-78 field program. The target area over which these studies have been carried out is shown in Fig. 1. This area will be referred to throughout this report when discussing the results of this study.

### B. Scientific Objectives

Certain specific tasks were set forth in the initially proposed satellite studies. These tasks were sometimes expanded upon or modified or deleted depending upon data availability and changing needs of the SCPP. A list of the major studies undertaken in this report are:

- 1) To determine the ability of geosynchronous digital satellite data to quantitatively measure cloud top temperatures (CTT) over the Sierra Nevada and SCPP target area. This includes determining percentage of time upper-level detached cirrus may interfere with observations. Using all available "cloud" truth data (i.e. aircraft, raobs, radar) the accuracy to which these CTT's can be measured from satellites will be determined.

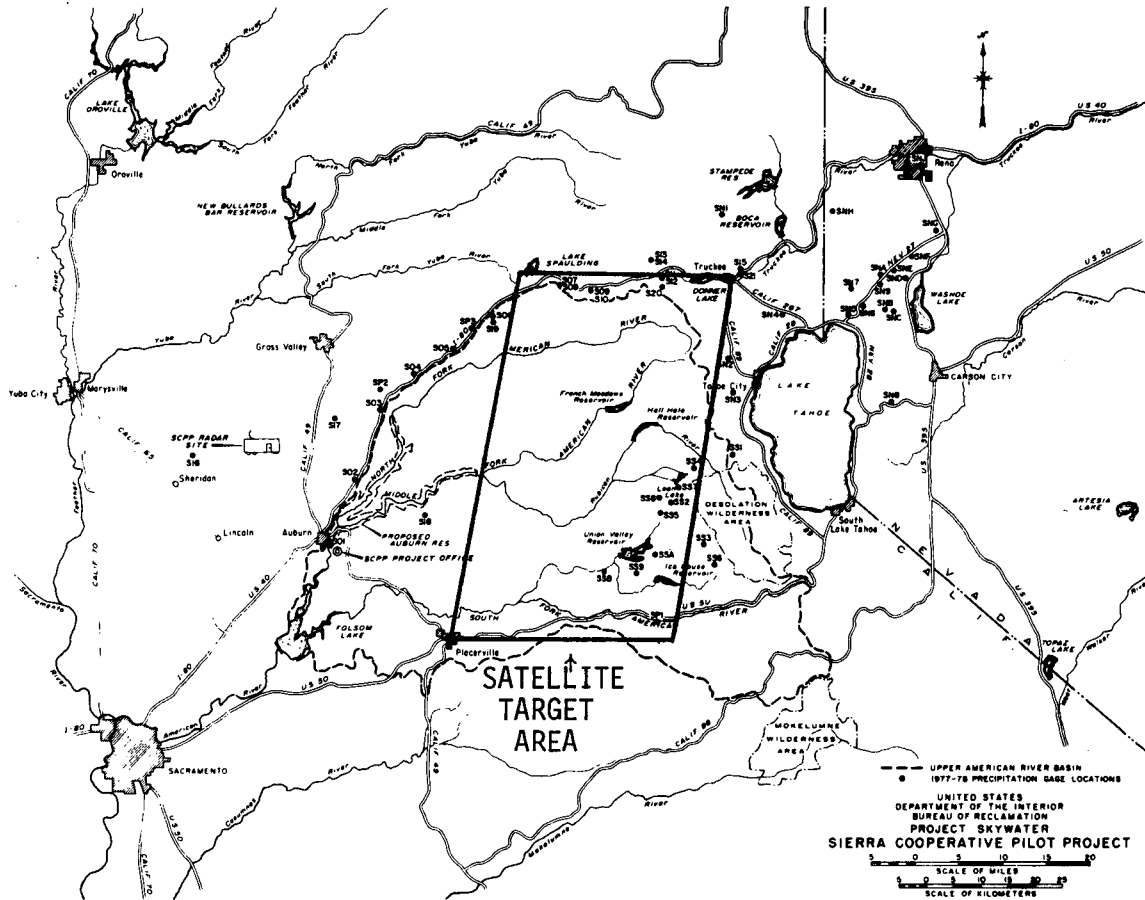


Figure 1. Map of SCPP Project Area. Radar and rawinsonde are located at Sheridan. Raingage locations referenced in this report compare to map locations S 01 to S 21 as follows:

S 01	Auburn
S 06	Blue Canyon (9 March 77 only)
S 09	PlaVada
S 12	Donner Summit
S 16	Sheridan
S 19	Blue Canyon
S 21	Truckee

2) Demonstrate the ability of the satellite imagery to observe convective band features within the overall storm system and their relative occurrence by storm.

3) Using available surface and upper air meteorological data stratify a storm sequence by cloud type, (i.e. convective, stratiform, etc.) temperature, and recommend from the satellite observations optimum periods of cloud seedability.

We believe that through use of the two years of available data, great strides have been taken in meeting these objectives. The following results document these advances, and should encourage the use of digital satellite imagery throughout the course of the SCPP.

## 2. SATELLITE OBSERVATION AND TECHNIQUES

### A. Geostationary Satellite Data for the Sierra Project

Digital satellite imagery for the 1976-77 and 1977-78 seasons of the Sierra Cooperative Pilot Project was from the SMS-2 (Synchronous Meteorological Satellite) stationed above the equator at 135°W. The SMS VISSR (Visible and Infrared Spin-Scan Radiometer) provides visible (0.55 to 0.70 micron band) and infrared (10.5 to 12.6 micron band) images each half hour in the normal operational mode. Satellite resolution over the Sierra target area for the visible channel is 1.34 km north to south by 0.84 km east to west. Because of the satellite-earth viewing configurations at different points on the globe, the north-south leg of the picture elements over the Sierra region is inclined at an angle of 10 degrees to the east of north.

Digital data for three storm periods in the first year and four in the second year were gathered from the Direct Readout Ground Station (DRGS) at the White Sands Missile Range, New Mexico. A nearly continuous sequence of half-hourly infrared and daytime visible digital images was received for these storms. In addition, up to 5 IR digital images per day for other storms during the first year were obtained from the limited archive of the National Environmental Satellite Service (NESS).

Only a limited geographical sector within the entire satellite full-disc image was recorded, and the areal coverage of a typical sector is shown by the image in Fig. 12. A listing of available data may be found in the 1976-77 and 1977-78 SSCP Data Inventories of the Bureau of Reclamation's Project Skywater.

## B. Navigation of Satellite Imagery

Small perturbations in the orbit of the nearly geostationary satellite cause features on the earth as seen by the satellite to drift through periodic displacement as the orbit progresses. Most of this movement is removed during the data transmission by using a set of parameters which describe the orbit. In this manner, a computerized grid is sent within the data stream so that features on the image can be located relative to the earth. The error in the location of this grid is often quite large, as is seen by comparing landmarks visible on the image to the grid position. This gridding, along with the use of landmarks, was used to co-locate the images and determine the position of the Sierra Project target area within them for the 1976-77 data set. When no landmarks were visible, in particular during the night when only IR images are available, the grid was the only way to navigate the first year's data. For the 9 March 1977 case study in this report, the grid appeared to be accurate to within 5 to 10 km.

A more accurate navigation is possible by using line documentation recorded at the beginning of each line of IR data in the 1977-78 data set. This method requires a satellite attitude to be determined by making landmark location measurements in terms of latitude and longitude on the earth, and line and element on the satellite image. Analytic navigation routines (Smith, Phillips, 1972) then give a "best fit" set of orbital parameters which combine with the scan number of the satellite VISSR to navigate the data in the line (north-south) direction. A "beta" parameter, which is derived by sensing the sun's and earth's edges by the satellite, is included in the line documentation,

and along with a single landmark measurement for the day, gives the navigation in the west-east direction along a scan line.

Navigation in this case means that the program returns the satellite line-element tape coordinates of desired earth locations for each image time. The 1977-78 data set is navigated by this method, and the accuracy of the method is generally within 3-5 km.

### C. Digital Image Display and Processing

#### L. The CSU ADVISAR

The ADVISAR (All Digital Video Imaging System for Atmospheric Research) at Colorado State University is a versatile digital data display and processing system. Eight solid-state memories under computer control are the basis of the system. Each memory stores an array of 512 x 512 eight-bit resolution elements, which are written at television refresh rates to a CRT. Both color and black and white monitors are the display end of the ADVISAR. 7 and 9 track tape drives and a disk allow permanent data storage and transfer back and forth from the memories.

The ADVISAR is an interactive system with a variety of controlling programs run from a terminal keyboard. These programs exploit the capabilities of the ADVISAR hardware to process and display digital data. Programs are on permanent disk storage and are accessed by the computer as they are needed. The computer drives all the peripheral devices of the system, thereby controlling the transfer and modes of display of the data.

### II. ADVISAR Capabilities

With 8 memory planes available, the ADVISAR can be used to create a movie loop type of display via the monitors. Memories can be

displayed with a choice of sequence and rate, and with geostationary satellite data permits motion and development of weather and other changing features to be easily observed.

Interaction with the digital data being displayed is by means of a joystick-cursor combination. Cursor size and position are set by positioning of two joysticks or can be defined exactly by keying in the parameters from the ADVISAR console. Cursor type, color and thickness are all variable. The cursor defines a precise point or area on the screen for many purposes. Digital values within the cursor may be output, zoomed or moved from memory to memory, be used in calculations, set to specific values, etc. Exact cursor location and size with respect to the memory array are accessible and are useful for locating features on an image.

Computer access to the memories is used for identification and removal of noise and missing or bad lines of data. Many examples of graphics capabilities are seen in the imagery examples within this report. Graphics are most useful for identification of displayed images and to point out interesting image features.

Shifting of images, up and down or left and right, aligns images precisely so that movement of features from one image to another can be determined or eliminated. Image overlaying displays two or more frames at the same time so that digital values in one frame need not be altered by the desire for grids, graphics, etc. to be displayed on an image. Overlaying also isolates moving or stationary features on multiple images as does digital image subtraction or addition, another capability. More complete descriptions of ADVISAR uses and capabilities are given by Brown (1978), Reynolds and Morris (1978a), Andrews and Fitch (1979).

### III. Color Enhancement of Digital Imagery

A most advantageous feature of the ADVISAR for the quantitative study of cloud top temperatures is its discrete color enhancement capability. Color enhanced digital imagery simultaneously reveals both the quantitative and qualitative aspects of the image, with minimal sacrifice being incurred by each. Enhancement assigns a shade of color to digital values or ranges of values upon output to the color monitors. In this way, colors on the image represent areas of given temperatures (for infrared images) or brightness (visible images). Fig. 9 is an example of a color enhanced IR image. Here it is easy to pick out the cloud areas and at the same time view the cloud top temperatures. While black and white enhancement can achieve the same effect, the inability of the eye to discern between shades of grey makes color enhancement much easier to decode quantitatively.

### 3. GENERAL CLOUD CHARACTERISTICS OF SIERRA STORMS

Before discussing the specific results of satellite studies for SCPP, a background study of the literature provided information on what is known about Sierran storms to date. This will allow comparison to conclusions based on the results of the present satellite studies to be given at the end of this report.

#### A. Convective Cells and Bands

Bands of convection imbedded in the large scale cloud mass are a common characteristic of California coastal storms during the winter (Fig. 30). The onshore movement of these bands has been studied by Elliott and Hovind (1964) and their characteristics of size, speed, etc. determined through the analysis of precipitation gage records from a coastal network. They found the bands to be 40 to 80 km wide, 60 to 120 km apart. Convective cells composing the bands moved relative to the bands towards lower pressure. Bands appeared to be oriented along the shear vector between the upper level of the convective region and the next level above the convection, while moving in the direction of the low level shear vector. Convective activity was related to increased instability within the storm due to differential temperature advection.

Radar has been used to track cloud bands from offshore into the Sierra during the CENSARE (Central Sierra Research) project which ran from 1968-1973 (Peace, 1975). One to six bands per group may occur, two or three bands being most common. Bands of 10 to 40 km radar width are spaced 40 to 200 km apart, with their observed length often being limited by the range of the radar itself. During large slow-

moving storms, two to three groups of bands may occur 12 to 24 hours apart. A cold front often follows the last band of each group.

The bands observed by radar are oriented north to south or northeast to southwest and are well organized offshore. In crossing the Coast Range they become somewhat disorganized, and reorganize upon reaching the Central Valley. Upon encountering the Sierra foothills, the northern end of the band slows until the band becomes parallel to the Sierra Nevada, oriented north-northwest to south-southeast. This is because individual cells in the line begin to curve cyclonically at the foothills until they are moving roughly parallel to the barrier. At this time, line echoes tend to break up into individual cells that climb the slope.

In the vertical, convective cells tend to be imbedded and extend upward out of a more shallow layer. At low scan angles, the cells are indistinguishable from the shallow layer at full radar gain. During CENSARE vertically-pointing radar showed no evidence of a layered structure in the detectable cloud, with only one exception where two layers were detected. Higher tops were found in warmer storms with higher precipitation rates. Finally, Peace found that echo movement was close to the 2500 to 3000 m winds aloft, and both showed cyclonic curvature nearing the Sierra crest.

Observations of mesoscale convective bands are not limited to California coastal storms. A very detailed study has been made of a continental occlusion in New England (Kreitzberg and Brown, 1970). Convective bands associated with both the warm and cold fronts contained cells which accounted for most of the precipitation in the system. In their study, warm frontal bands were attributed to tongues

of warm moist air, over the frontal surface aloft, being overrun by cooler air and breaking out into convective bands within the stratus deck. Ahead of the cold front, bands were associated with a prefrontal surge of cold air and behind it, with the cold front itself. Again, the bands were oriented along the shear vector as in the Pacific Coast storms above. This orientation also parallels the surface front with which the bands were associated.

Additional studies by Matejka et al. and Hobbs et al. (both 1978) confirmed the results of Kreitzberg and Brown while also relating the mesoscale features to cloud microphysics and precipitation efficiency. One result of Hobbs et al. which differs from those of Elliott and Hovind, and Kreitzberg and Brown, is in the speed and direction of motion of prefrontal bands and cells. Hobbs et al. found the motion to be similar to, not to the right of, the winds between 3 and 6 km, near the upper level of the convection. Their aircraft flights show that large amounts of supercooled water exist within the cells, an important finding for weather modification purposes.

#### B. Sierra Orographic Clouds

Rainfall records within the Sierra range point to the orographic enhancement of precipitation on the upwind side of the barrier (Lamb et al., 1976). While the effect on precipitation may be the same as for inland mountains such as the Rockies, it has long been realized that the winter orographic clouds for the two are very different. The average Sierra storm is much wetter and warmer than continental storms, due to the proximity of the Pacific Ocean, the onshore flow during storm events, and the relatively low elevation of the upwind Central Valley.

The concept of a smooth orographic cloud does not apply here; convective instability in the low level moist layer is released as air is forced to rise up the barrier. Aircraft flights during winter storms of 1971-72 and 1972-73 were taken to measure cloud liquid water across the Sierra (Lamb et al., 1976). A strongly convective region, as revealed by turbulence, with high liquid water content was found from 40 to 75 km upwind of the main crest. Surface precipitation was greatest at a distance of 10 to 30 km upwind of the crest, with particles growing in the convective region and falling to the ground some distance nearer the crest. Downwind of the convective zone and beyond the crest, much less cloud activity and little surface precipitation was found. Convective overturning was found to occur in both frontal and post-frontal situations, as the barrier restricts low level flow more than at higher levels.

Marwitz et al. (1978) have found that a post-frontal convective cloud wall, where upwind and downwind regions are mostly clear, is common after a cold front. Located upwind of the crest over the foothills, this cloud wall is truly orographic in the sense that its existence is due solely to the presence of the Sierra. Their aircraft flights have shown these clouds to have the most supercooled water and least ice crystals of all clouds during a storm's lifetime over the Sierra.

#### 4.0 INTENSIVE CASE STUDIES

##### 4.1 9 March 1977 CASE STUDY

The 9 March storm was one of the few significant storms that occurred in the drought-stricken winter of 1976-77 in California. A deepening middle-level trough formed along the West Coast in response to strong cold advection to its rear. Pre-frontal precipitation was falling over the mountains from a fairly warm ( $-10$  to  $-15^{\circ}\text{C}$ ) orographic cloud at 0945 GMT. The main part of the storm swept through southern Oregon. As a result, no extensive high cloud covered the frontal band in the target area.

Decreasing CTT preceded the surface cold front as the frontal cloud band entered the target (Figure 2). Coldest cloud tops over the target were at 1445 just before the front, where mean CTT in the target was  $-33^{\circ}\text{C}$  and the coldest cloud element seen in the target was  $-38^{\circ}\text{C}$ . Radar observed cloud tops agreed fairly well with the satellite cloud tops.<sup>1</sup> The radar top of  $-41^{\circ}\text{C}$  at 1530 GMT was not verified by the satellite (Figure 2), due to the lower resolution of the satellite IR sensor averaging out this small perturbation.

Precipitation began increasing sharply around 1345 at Plavada to a maximum of 9 mm per hour with the frontal passage (Figure 3). No rain fell at Auburn in the Central Valley until the frontal band passed over. Precipitation rates at all stations shown in Figs. 3 and 4 are closely related to the decreasing target area CTT. In a storm such as this one, the above result is to be expected. The decreasing CTT is

---

<sup>1</sup> Using the Sheridan sounding the satellite cloud-top temperatures could be converted to km above mean-sea level and the radar heights could be converted to temperature for comparisons.

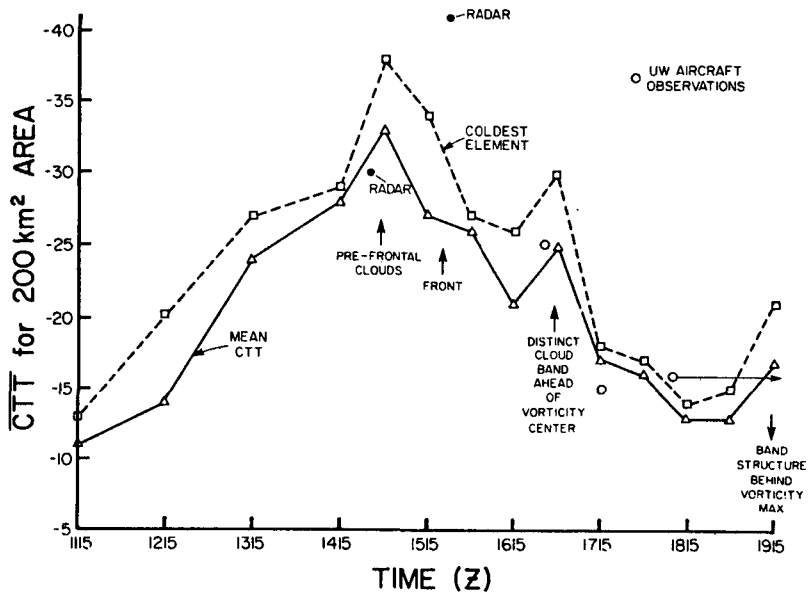


Figure 2. Satellite-observed CTT, 9 March 1977.

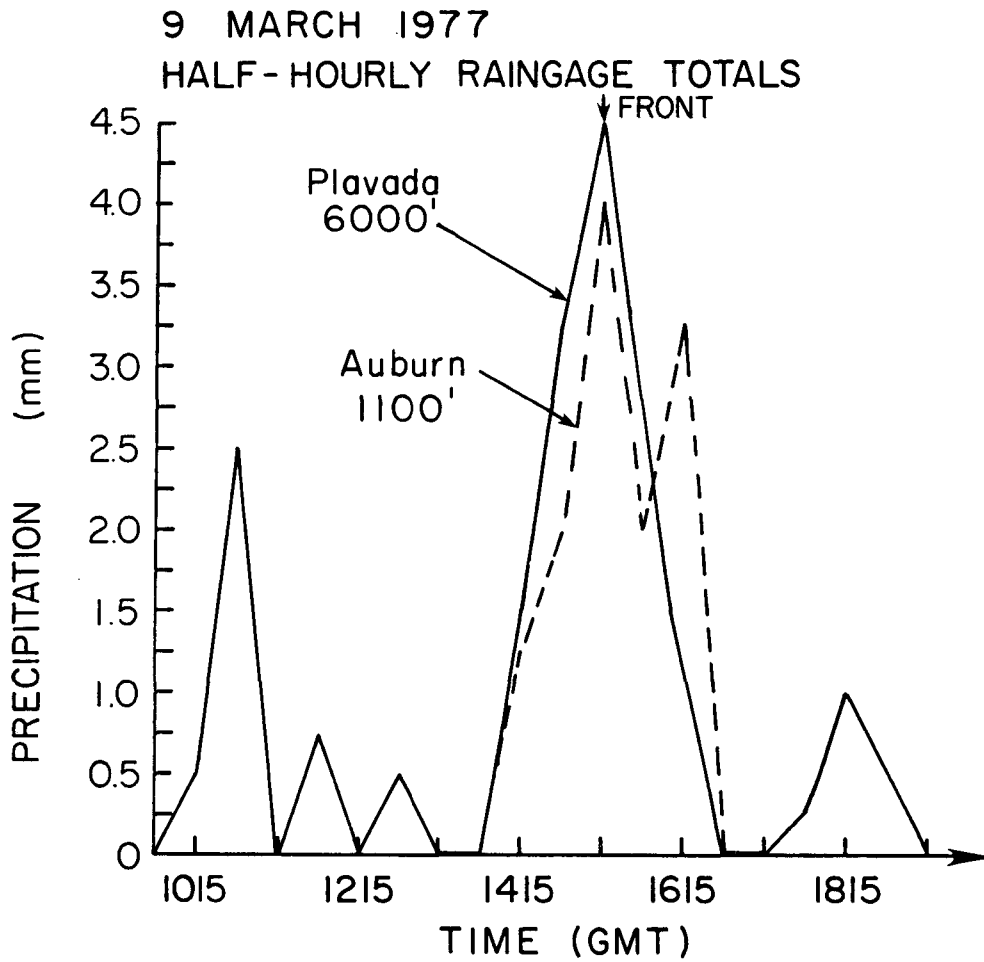


Figure 3. Raingage records for PlaVada and Auburn, 9 March 1977. Time of frontal passage is shown.

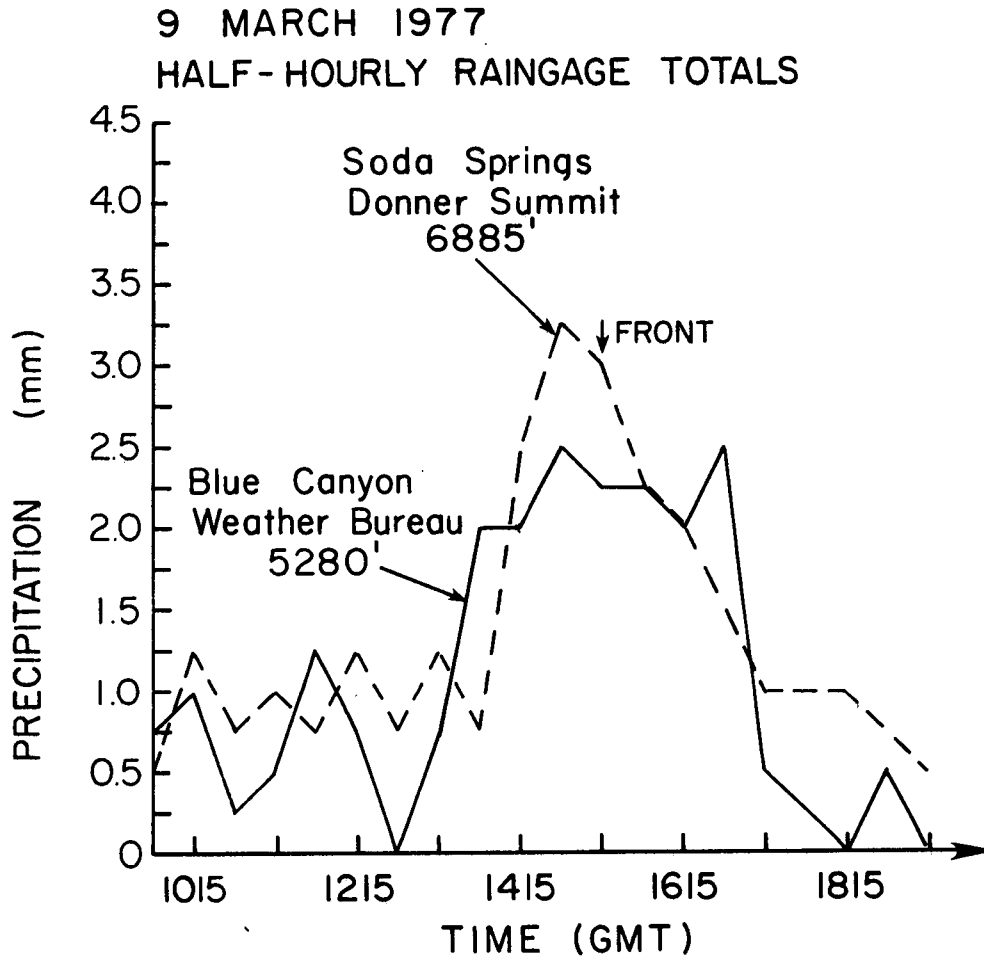


Figure 4. Raingage records for Blue Canyon and Donner Summit, 9 March 1977. Time of frontal passage is shown.

not due to overlying cloud cover with the front, but to deeper clouds due to convergence and thus increased processing of available moisture.

Within the large frontal band, narrow bands of enhanced convection were seen (Figure 5). The band just on the southeast corner of the target in this image affected mean CTT and Auburn and Blue Canyon precipitation at 1645 GMT. Another band to the north, partly covered by cirrus, arrived at the project area near 1900 GMT. Forced by the upper trough and not the surface front, this band's CTT approached  $-50^{\circ}\text{C}$ . Covered by smooth cirrus, the convective elements of the band were hidden from satellite view.

The 9 March storm provided good observations of a cold frontal passage through the Sierras. Observations of this storm clearly showed the decrease in CTT ahead of the front to a value below the lower boundary of the seeding window ( $-25^{\circ}\text{C}$ ), during which most of the precipitation took place. Pre-frontal and post-frontal CTT of the orographic cloud remained well within the seeding window, with the cap cloud dissipating several hours after the frontal passage. Reynolds (1977) and Reynolds and Morris (1978 a,b) include descriptions of the 9 March, 1977 storm. Radar observations of the storm are summarized in Sutherland et al. (1977) and agree well with the satellite results. Radar observed the frontal band merger into the orographic cloud and also detected the post-frontal band within the target area as seen on the satellite image at 1645 GMT.



Figure 5. 1715 GMT, 9 March 1977 visible image. Narrow bands of convection are seen within the cloud mass. Satellite target area is within the cursor box.

#### 4.2 14-15 December 1977 CASE STUDY

A large 50 kPa trough in the Gulf of Alaska with strong westerly flow into the California coast above 70 kPa existed on 14-15 December. 20 and 30 kPa flows were fairly zonal from the central Pacific into the Sierra during this storm, with a strong jet axis just north of the latitude of the target area. A vigorous short wave trough at middle levels, emanating from the Aleutian low, passed over northern California after 1200 GMT on 15 December. Figure 6 is a composite of the 50 and 70 kPa observations for 1200 GMT, 15 December showing the strong westerly flow into the Sierra near the time of frontal passage.

Features of the 14-15 December storm worth noting are many in number. In comparison to many winter Sierran storms this one was warm, with rain falling at elevations up to 2400 m early in the storm. Precipitation at Blue Canyon is strongly related to cloud top temperature in the target area. The major precipitation event is forced by increased low-level upslope winds 6 hours in advance of the front, during a period of clearing high clouds. Another sharp drop in cloud height follows the frontal passage, typical of most of these storms. An isolated orographic cloud remained over the Sierra behind the front. It lasted for several hours, producing showery precipitation due to its convective nature. At this time, CTTs ranged from  $-15$  to  $-20^{\circ}\text{C}$ . Moore (1978) gives a more complete description of the synoptics and microphysics of this storm.

In the pre-frontal environment on 14 December, multi-layered clouds were evident from project soundings up to 1800 GMT and were also observed by University of Wyoming aircraft flights. By 2100, no cloud layering was seen on the soundings and satellite observed CTT had fallen

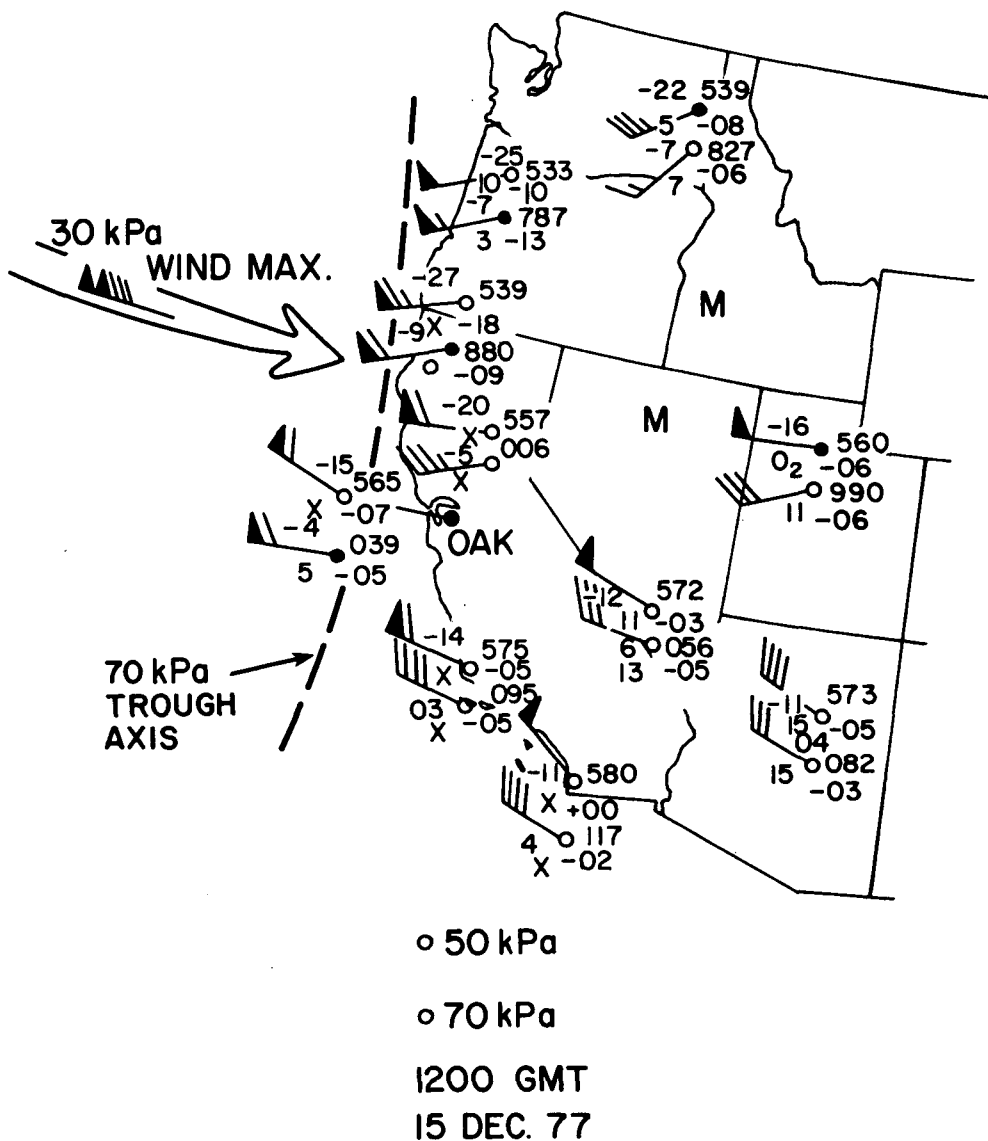


Figure 6. Composite 70 and 50 kPa observations, 1200 GMT, 15 December 1977. 30 kPa jet max is shown.

to  $-40^{\circ}\text{C}$  in the target (Figure 7). Blue Canyon precipitation increased after 2100 with the decreasing CTT, yet remained marginal at Donner Summit (Figure 8). As a slight break in high cloudiness passed over the region, the increased CTTs were accompanied by a decrease in Blue Canyon precipitation totals at 0045 GMT, 15 December. CTT again decreased as cloudiness associated with the lifting ahead of the trough passed over the target. A secondary maximum of precipitation occurred at Blue Canyon, centered around 0315 GMT under the coldest clouds of the entire storm period. It is difficult to determine whether layered cloudiness was present from the 0300 Sheridan sounding, on which the relative humidity decreased smoothly with increasing height. The good relationship between observed CTT and Blue Canyon precipitation after 0300 GMT would indicate that a microphysical connection between the cirrus and lower clouds was taking place, inferring natural seeding.

Heaviest precipitation fell at around 0600 GMT on 15 December at both Blue Canyon and Donner Summit (Figure 8). At that time, a strong low-level jet appeared at 85 kPa on the Sheridan sounding, from  $225^{\circ}$  at  $26\text{ ms}^{-1}$ . The strong orographic component to the low-level winds combined with abundant moisture to produce the observed precipitation. CTT increased during this time from  $-40^{\circ}\text{C}$  to  $-30^{\circ}\text{C}$ , warming to  $-25^{\circ}\text{C}$  by 0745. Figure 9 is the 0445 GMT IR image showing the cold, high clouds moving off to the east of the Sierra, with an extensive orographic cloud remaining behind.

With the approaching cold front, precipitation increased moderately at Donner Pass and significantly at Blue Canyon, up to 1145 GMT. After frontal passage between 1215 and 1245 GMT, cloud heights and precipitation rates decreased sharply due to subsidence behind the front. A

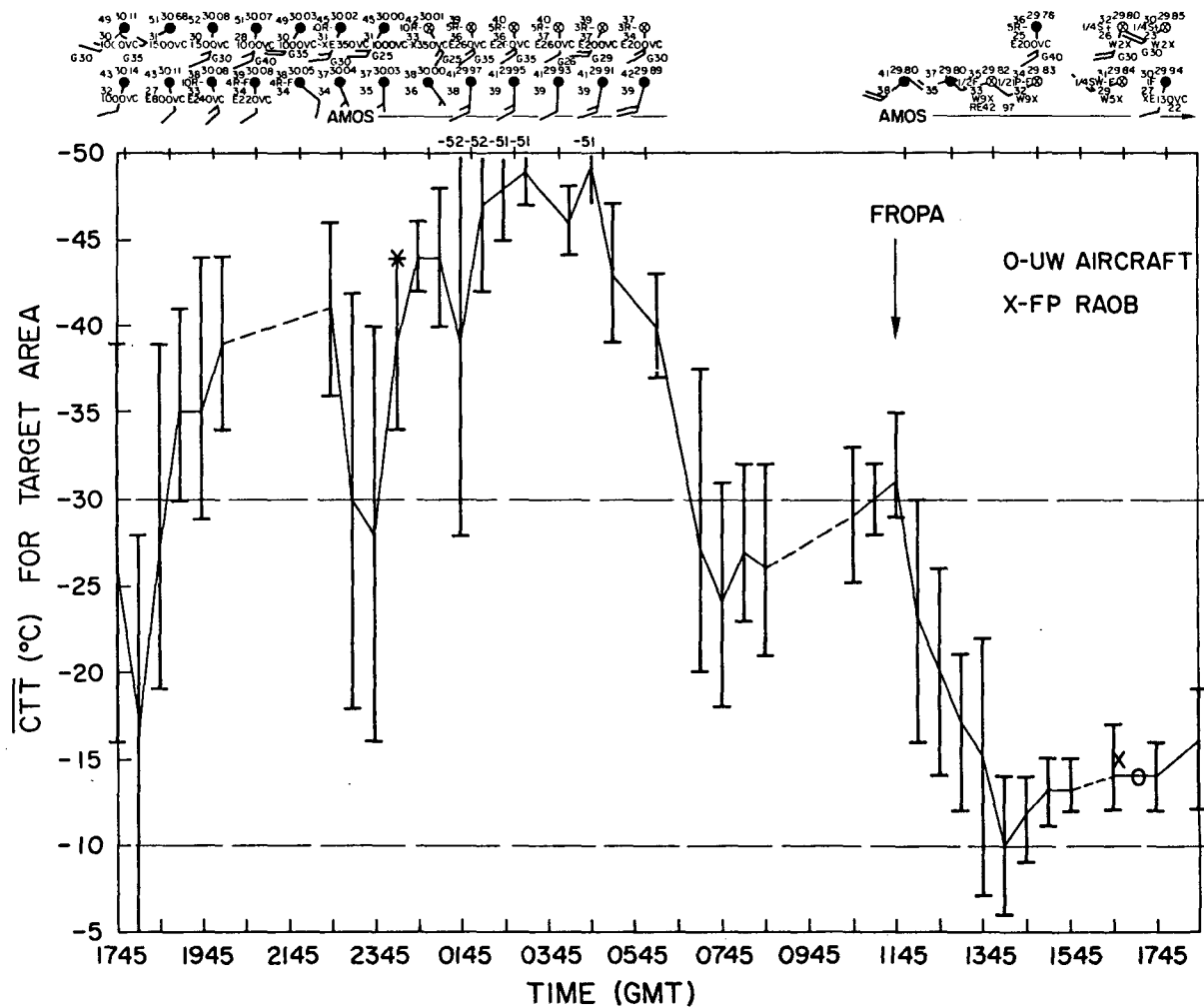


Figure 7. Satellite-observed CTT, 14-15 December 1977. Dashed lines indicate missing data.

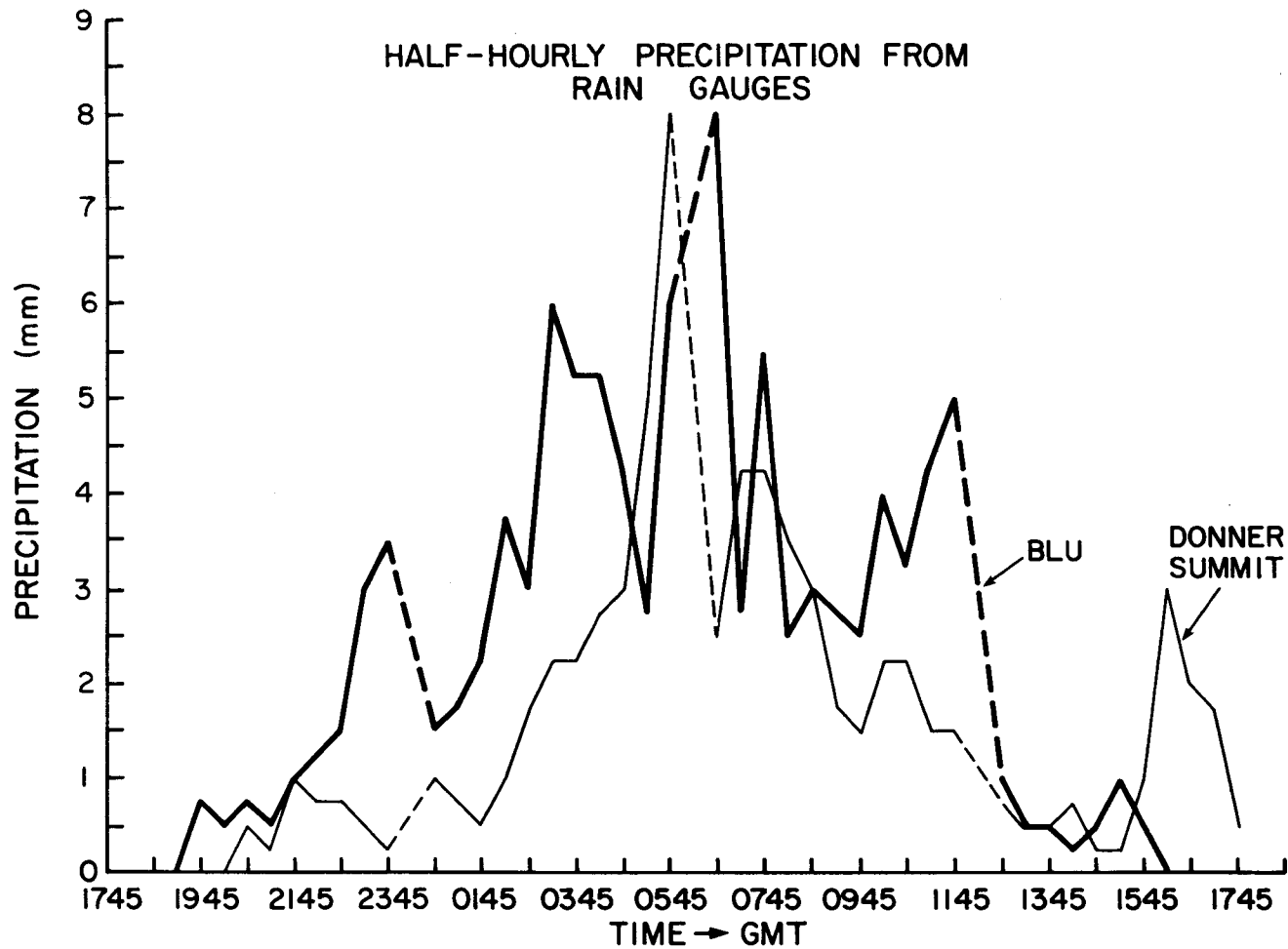


Figure 8. Raingage records for Blue Canyon and Donner Summit, 14-15 December 1977.

Figure 9.

0445 GMT, 15 December 1977 IR image.  
Black areas are cloud tops colder than  
-50°C. Color key at top gives CTT  
coding.

Figure 13.

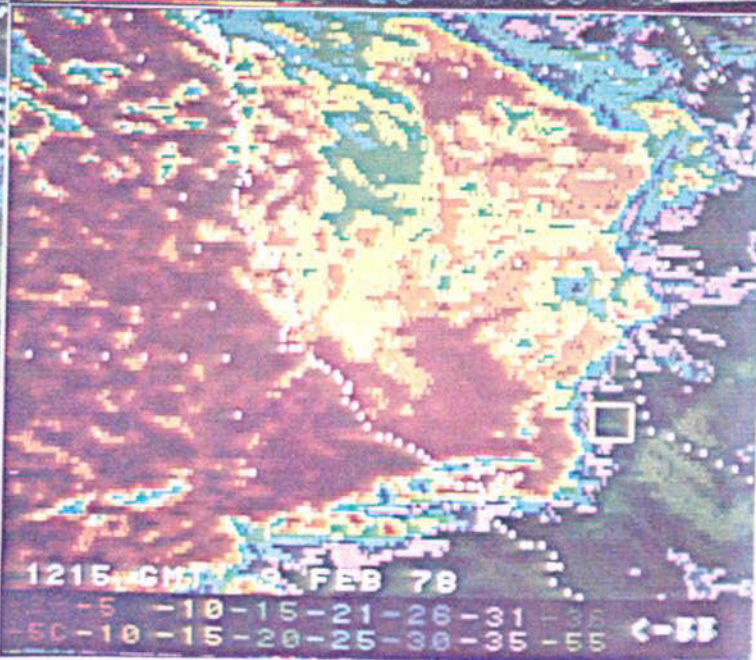
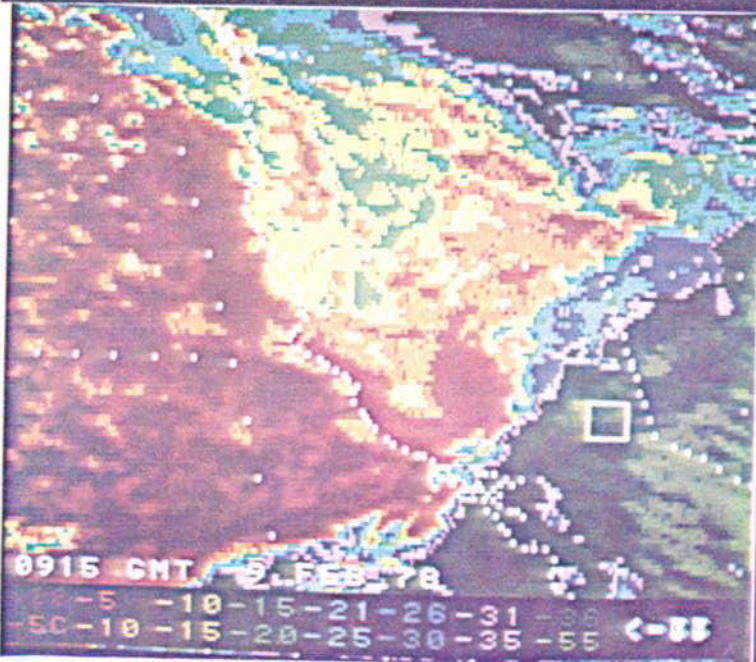
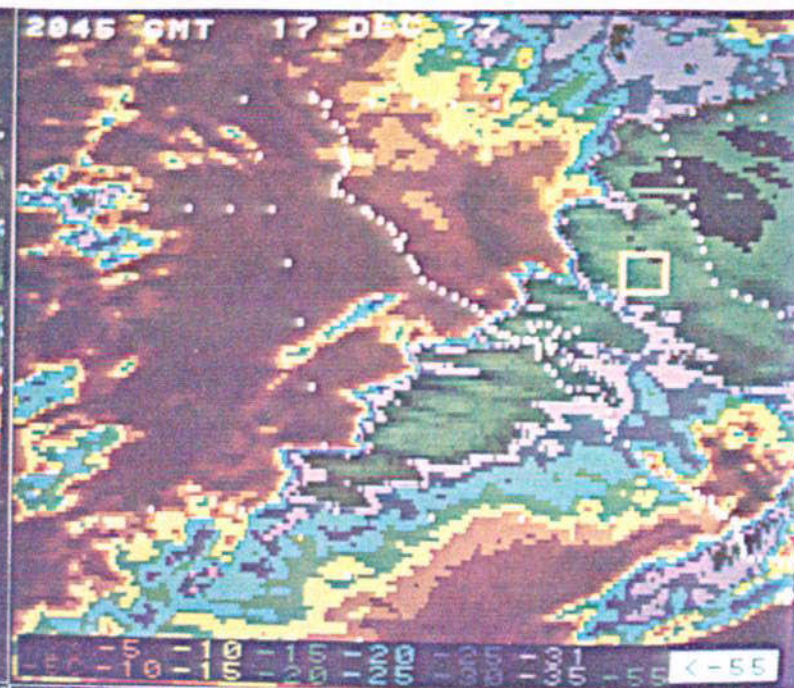
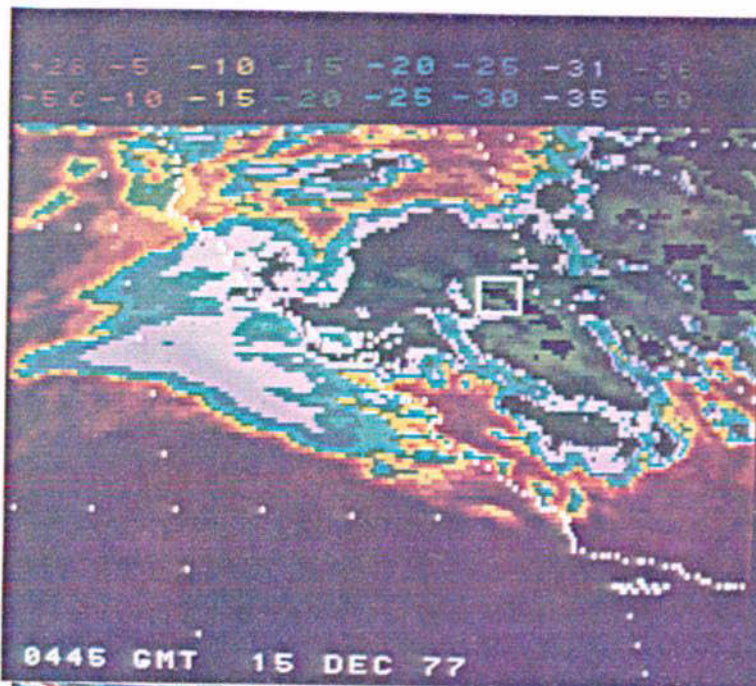
2045 GMT, 17 December 1977 IR image.  
Cold front lies within the target  
area; cirrus extends nearly 100 km  
to the northwest behind the front.

Figure 17.

0915 GMT, 9 February 1978 IR image.  
Front is approaching target area.  
Frontal band and Sierra orographic  
cloud are visible as colder bands  
in the cirrus (lighter shades of  
green). May imply that cirrus and  
lower clouds are contiguous.

Figure 19.

1215 GMT, 9 February 1978 IR image.  
Compare cloud cover to analyzed  
frontal position in Figure 18.



precipitating orographic cloud with CTTs of  $-15^{\circ}\text{C}$  to  $-20^{\circ}\text{C}$  persisted more than 8 hours after frontal passage. A pocket of moisture near 80 kPa seen on the 1800 GMT Sheridan sounding may have accounted for some of the Donner Summit precipitation peak around 1615 GMT, along with increased convective instability as cold air intruded above the station.

#### 4.3 17-18 December 1977 CASE STUDY

Upper winds were fairly zonal in the eastern Pacific and western U.S. on 17-18 December, but less so than during the 14-15 December case. A short wave embedded in the flow was just off the California coast at 0000 GMT on 18 December. At the surface, a cold front passed the target area around 2115 GMT on 17 December in advance of the upper wave. Ahead of the front, a wide band of cloudiness covered with cirrus moved over the target area, giving satellite-observed CTTs around  $-44^{\circ}\text{C}$  at 1545 GMT (Figure 10). At 1500 GMT, the Sheridan sounding had approximately a 1300 m separation between upper and lower clouds with the separation centered near the 57 kPa level. Mean CTT of the lower deck was  $-12^{\circ}\text{C}$  and of the upper deck was  $-41^{\circ}\text{C}$  in the target area. A separation between cloud decks lowered by 1800 GMT as precipitation began to increase with the approach of the cold front (Figure 11). By 1845, over 8 mm per hour rain rates were occurring at Blue Canyon. Precipitation rates at Truckee and Donner Summit peaked about an hour later, just ahead of the front.

The frontal band of cloudiness is seen on the 1945 GMT visible image, Figure 12. The band itself was moving to the southeast with the cold front. The clouds comprising the band moved from the west-southwest with the upper winds. Slight troughing off the coast at 20 and 30 kPa was responsible for the cirrus which covered the frontal band and flowed in off the Pacific continuously, parallel to the surface front.

High clouds did not clear out with the passing front in contrast to most days studied. The 2045 GMT IR image (Figure 13) revealed the extent of cirrus cover behind the front, which was just within the target area at this time. With frontal passage at 2115 GMT, it was seen

17-18 DEC 1977

MEAN AND STANDARD DEVIATION OF CTT OVER TARGET AREA

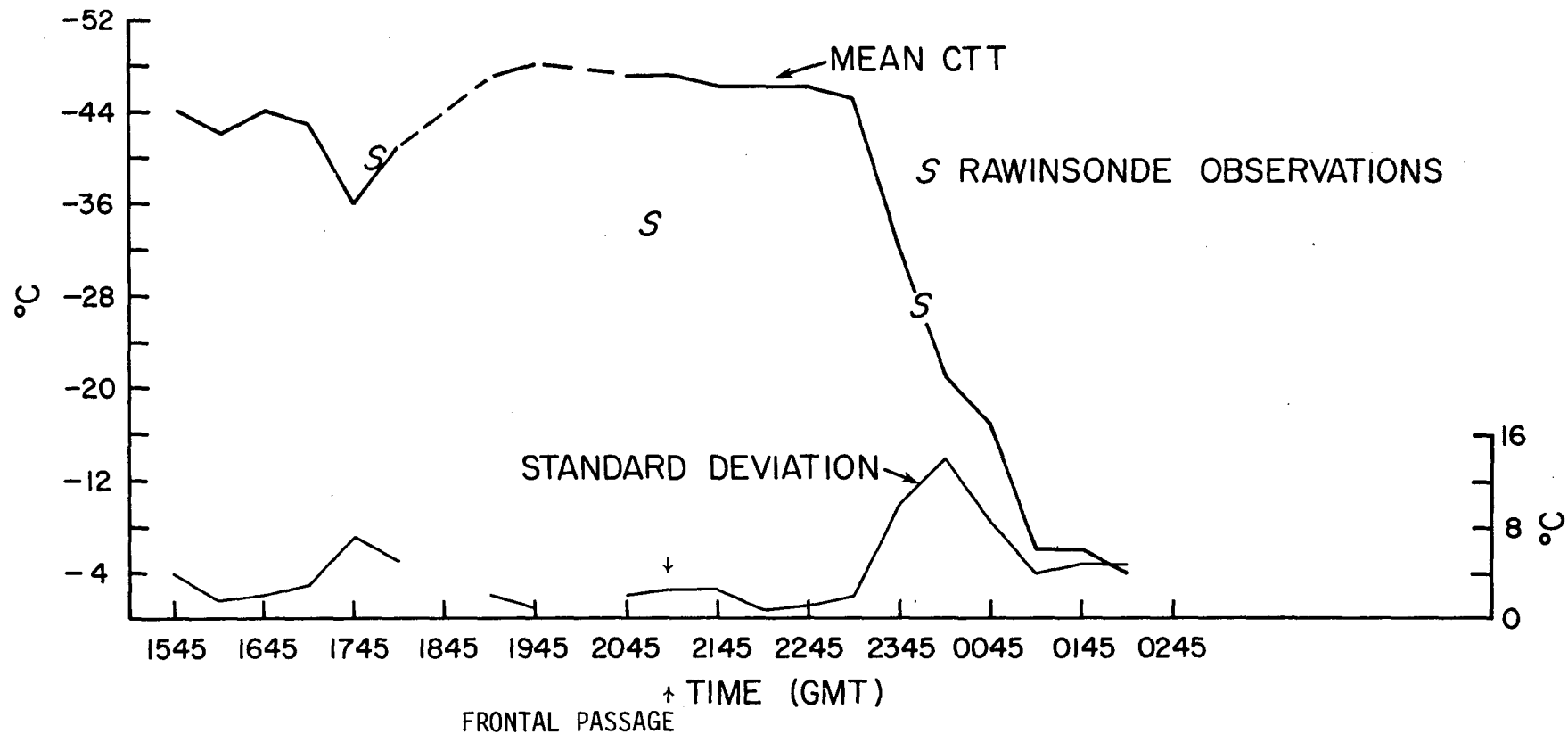


Figure 10. Satellite-observed CTT, 17-18 December 1977.

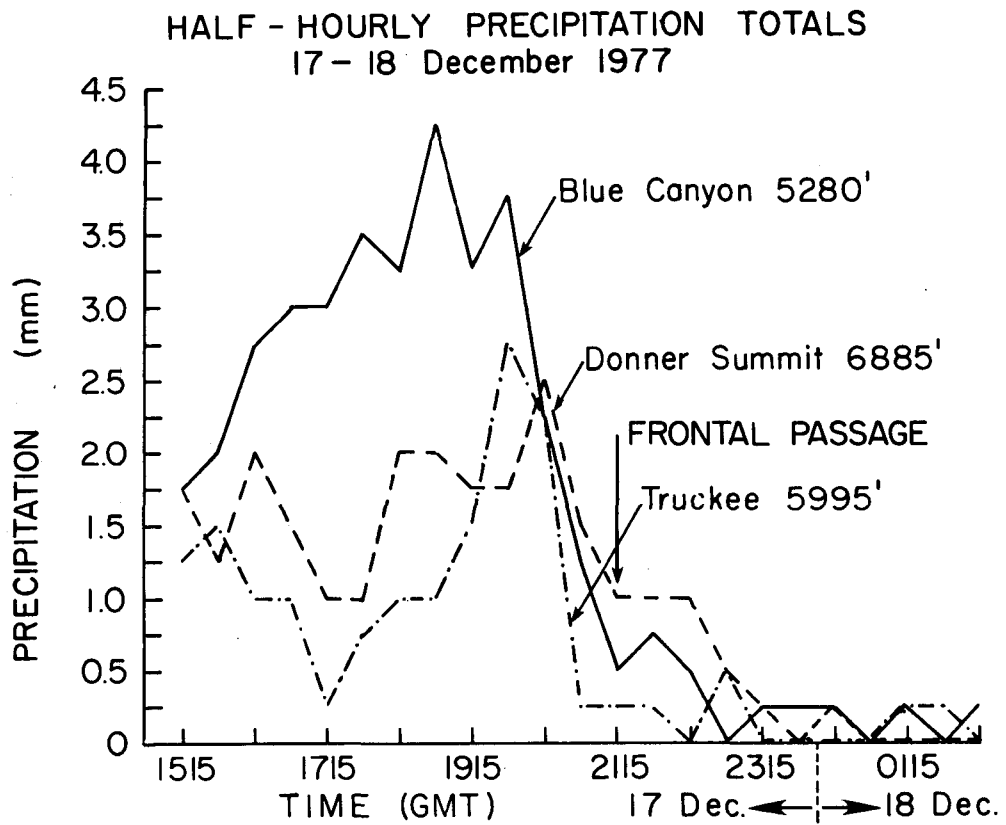


Figure 11. Raingage records for Blue Canyon, Donner Summit and Truckee, 17-18 December 1977.



Figure 12. 1945 GMT, 17 December 1977 visible image. Front is northwest of the target beneath the cirrus cloud mass. Offshore banded structures is cirrus wave bands, not convection.

that the cirrus took 2-1/2 hours longer to pass over the target, doing so at 2345. The last of the significant precipitation fell just before the high cloud moved off (Figures 10 and 11). By 2100, the Sheridan sounding was dry below 80 kPa with the front having passed there. Due to the orientation of the front, almost perpendicular to the Sierra, the post-frontal orographic cloud and lifting were slight, and it appeared that mountain precipitation behind the front was from a middle to upper level cloud above 78 kPa.

Natural seeding from the upper cloud appears to have occurred during the time of heaviest precipitation, as the soundings showed the mid-level cloud separation to shrink and disappear by 2100 GMT. If this is the case, the satellite-observed CTT remaining very low (below  $-40^{\circ}\text{C}$ ) would indicate little potential for positive seeding results in this storm, with no warmer orographic cloud remaining after the front passed.

#### 4.4 8-9 February 1978 CASE STUDY

Atmospheric circulation was very strong in the Pacific during the second week of February. A deep low pressure system at 70 kPa moved southward from the Gulf of Alaska and passed over California between 0000 GMT and 1200 GMT on 9 February. The long wave trough at 20 and 30 kPa deepened off the west coast of the U.S. and heavy rains with flooding and mud slides occurred in southern California in the days following the Sierra storm.

Extensive thick cirrus on the southeast side of the long wave trough covered the target area over the lifetime of the storm, reducing the usefulness of satellite observations for identification of mesoscale features in the clouds. The 2245 GMT, 8 February visible image, Figure 14, shows the large areal coverage of upper level cloudiness preceding the trough. CTT was around  $-40^{\circ}\text{C}$  over the target at this time (Figure 15). From the 0000 GMT, 9 February sounding at Sheridan, the tops of upper level clouds were near 30 kPa. Winds at this level were from  $240^{\circ}$  at  $94\text{ ms}^{-1}$ . The high speed of the cirrus imbedded in the upper level jet was the most obvious feature seen in the satellite image loops displayed on the ADVISAR.

University of Wyoming aircraft observations between 1910 and 2220 GMT reported overcast skies above the low-level clouds, and no attempt was made to fly to the upper deck. Lower clouds were thus effectively blocked from the satellite view, with a gap between cloud layers from 85 to 53 kPa observed on the 2100 GMT, 8 February Sheridan sounding.

Precipitation began around 0000 GMT on 9 February at the mountain stations (Figure 16) and rain was reported at Sheridan, where a marked change in the sounding at this time took place. The gap between low

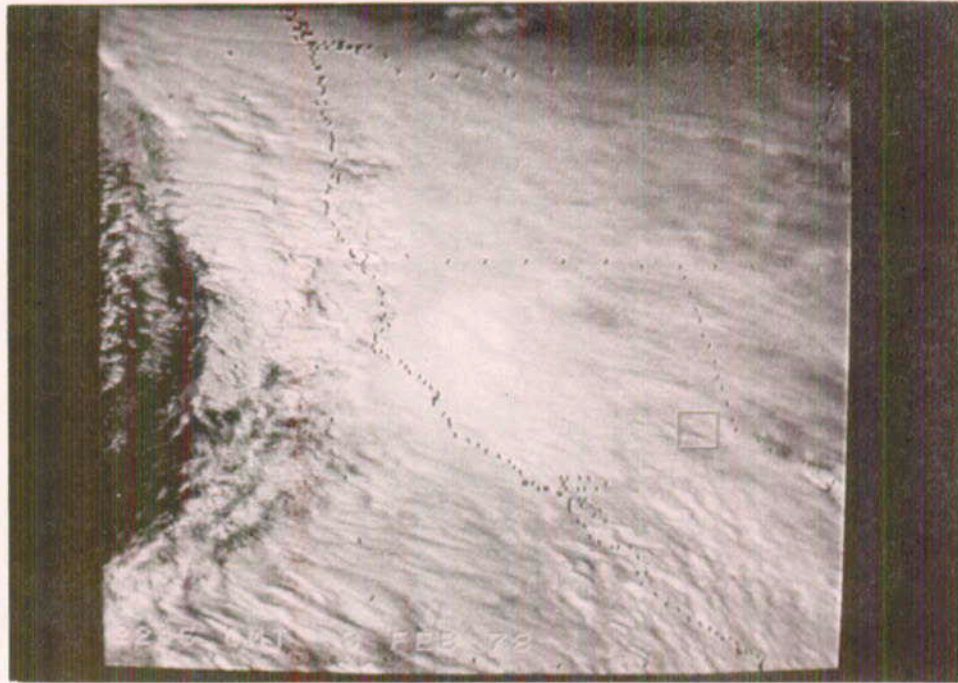


Figure 14. 2245 GMT, 8 February 1978 visible image. Cirrus covers California in the pre-trough situation.

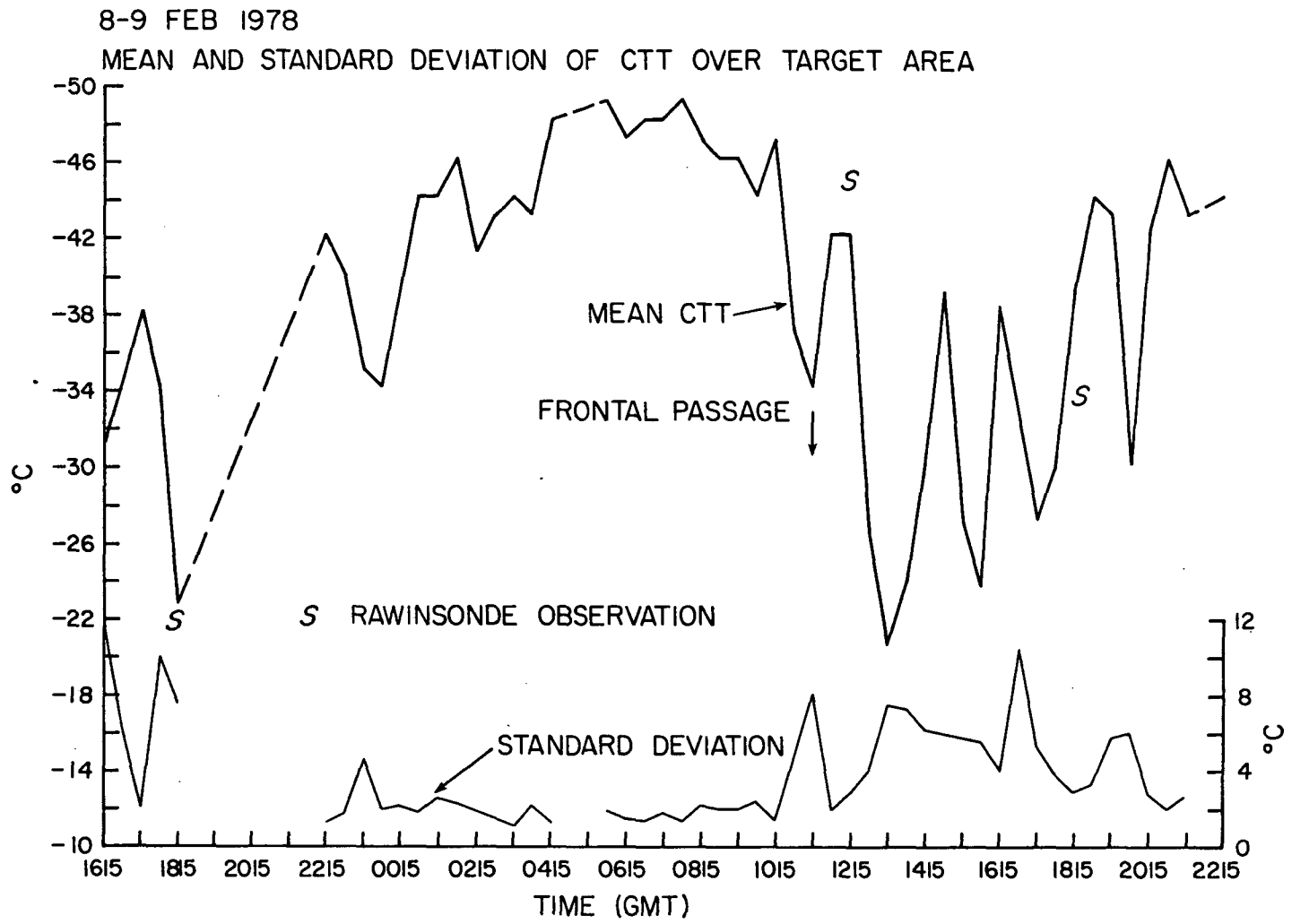


Figure 15. Satellite-observed CTT, 8-9 February 1978.

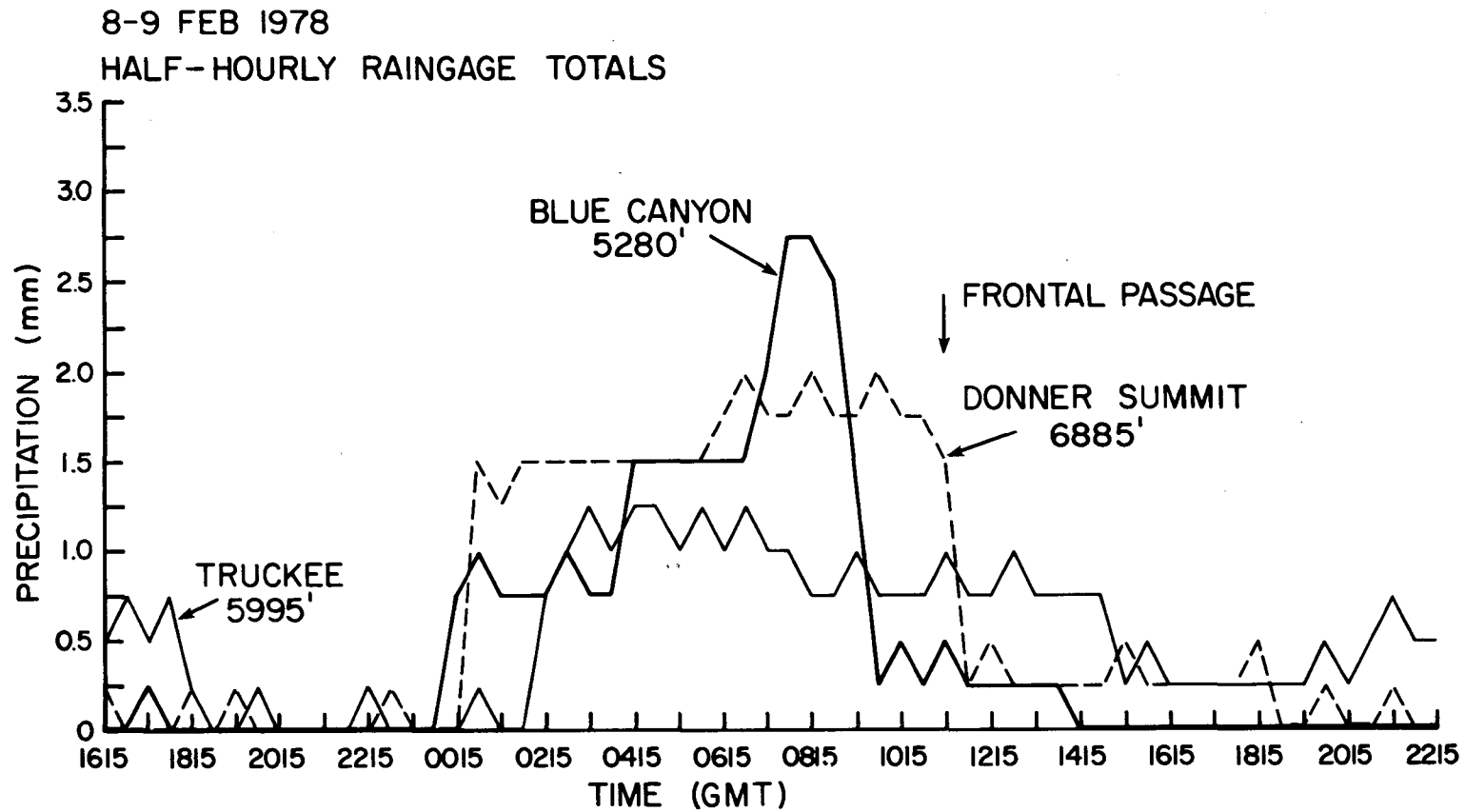


Figure 16. Raingage records for Blue Canyon, Donner Summit and Truckee, 8-9 February 1978.

and high clouds disappeared at middle levels, with warm, moist air having intruded, giving continuous clouds in the vertical as detected by rawinsonde. Stability increased in the 85 to 70 kPa layer but the air below 85 kPa was conditionally unstable yet drier than within the stable layer.

The main surface low pressure center stayed offshore from British Columbia throughout the duration of the storm. A cold front extended far south of the low into northwest California and beyond as precipitation began. Some distance behind the cold front, clearing out of the overlying cirrus shield occurred along a ragged cloud edge seen in the satellite images.

Precipitation increased as the front approached the target and was fairly steady with time. As the front progressed eastward, a secondary low formed on it along the northern California border, moving into northwest Nevada by 0900 GMT with the cold front. A strong southerly low-level jet with winds of  $25 \text{ ms}^{-1}$  at 600 m preceded the front on the Sheridan soundings prior to 0900 GMT. CTT was lowest during this time and except on the 0000 GMT sounding, a 1 to 2 km gap between the upper and lower cloud decks was present. Most of the precipitation fell prior to frontal passage during the time of the low-level jet. A lack of heavily precipitating convective cells is indicated by the precipitation records in Figure 16. The orographic precipitation was enhanced after 0700 GMT at Blue Canyon and Donner Pass near the time of frontal passage. The precipitation rate at Truckee, on the downwind side of the crest, was unaffected by the passing of the cold front.

Southern reaches of the cold front extending offshore into the Pacific from south-central California didn't progress eastward as did

the northern portions. As a result, the front became oriented north-east to southwest, nearly stationary south of the target area after 1500 GMT. Cirrus cover became similarly aligned as seen on the IR image at 0915 GMT (Figure 17) when the front was in the target area. Exact time of the surface frontal passage is uncertain, occurring some time between 0900 and 1100 GMT depending on the station observations used. The low-level jet disappeared from the 0900 GMT Sheridan sounding and Blue Canyon precipitation rate slowed at the same time. Donner Summit, at a higher altitude, continued in moderate precipitation until 1100 GMT.

The frontal position at 1200 GMT is shown on the NMC surface analysis, Figure 18. It appears that the front may still be north of Merced instead of in the position analyzed, but in either case, the 1215 GMT IR image (Figure 19) shows that the cirrus cover extended 100 km or more behind the front. The slow movement of the front, with another low forming on it offshore, was reflected in the slow southward migration of the cirrus edge which stalled over the target area. Sharp changes in CTT over the target (Figure 15) were caused by "dips" in the cirrus edge, such as in Figure 19, leaving the target area in and out of cirrus cover as the edge meandered back and forth. Mean motion of the cirrus was from the southwest, parallel to the edge of the cirrus, as indicated on the visible image at 2045 GMT (Figure 20).

While little significant precipitation fell in the target area after the frontal passage, there was significant rainfall under the cloud mass to the south. During the 24 hours ending at 1200 GMT, 10 February over 50 mm of rain fell near Fresno and Los Angeles as the low pressure center moved onshore into southern California along the front, causing flood conditions in some areas.





Figure 20. 2045 GMT, 9 February 1978 visible image. Arrow indicates movement of cirrus cover, parallel to its edge.

#### 4.5 2-3-4 March 1978 CASE STUDY

##### A. General Description

The storm sequence of 2-3-4 March was a very different storm in relation to those which have been discussed previously. From a satellite point of view, the obvious difference was the structure of the convective lines which moved onshore during this storm. Convective bands associated with the cold fronts had the appearance of squall lines, where large individual cumulonimbi made up the major portion of the band and could be followed for long periods of time.

Upper air charts showed a nearly stationary closed circulation off the coast of northern California which persisted throughout the observing period. Transient short waves passed through this system and accounted for most of the significant weather over the storm's lifetime. Moist southwesterly flow and precipitation in the mountains were almost continuous.

Two major cold fronts passed the project area about 40 hours apart. The cloud bands associated with these fronts were very dissimilar and will be described in detail in the following sections.

The length of this storm and the multitude of features associated with it have afforded many opportunities for the comparison of results obtained in this study to the results of earlier studies mentioned in the introductory sections of this report. These results are not strictly limited to Sierran cloud systems; offshore studies are included as well.

## B. 2 March 1978

Digital satellite data for March 2 began at 1545 GMT. At this time, precipitation was falling within the target area from a pre-frontal orographic cloud situated over the Sierra. Moist southwesterly flow into central California at lower and middle levels was present in advance of an offshore cold front associated with a short wave at 50 kPa. Mean CTTs over the target area in advance of the front were near  $-30^{\circ}\text{C}$  as measured by the satellite. The 1800 GMT sounding at Sheridan was moist up to this level, making it nearly certain that the lower orographic cloud was continuous up to the cirrus layer. Figure 21 shows a time plot of cloud top temperature, along with aircraft and rawinsonde observations of CTT. Aircraft CTT was from the North American Weather Consultants on-top airplane and is derived by comparing the measured height of the cloud top to the Sheridan rawinsonde. The apparent poor relationship between the satellite and aircraft-measured CTT can be partially explained by two factors: first, the locations of the aircraft measurements were mostly outside the satellite target area, usually in the upwind valley, and the temperature measurements were not made directly. Second, the satellite CTT plotted is an area average for within the target, so individual spots can be warmer or cooler than shown in the figure. The standard deviation of CTT in the target, also plotted in Figure 21, shows this variation.

A large, well-defined band of convective cells was associated with the surface cold front. At 1815 GMT the band encountered the California coastline. The 1915 GMT visible image, Figure 22, shows the frontal band onshore along the coast, while the valley to the east is clear. Over the target area, cirrus still covered the precipitating orographic cloud.

2-3 MARCH 1978

MEAN AND STANDARD DEVIATION OF CTT OVER TARGET AREA

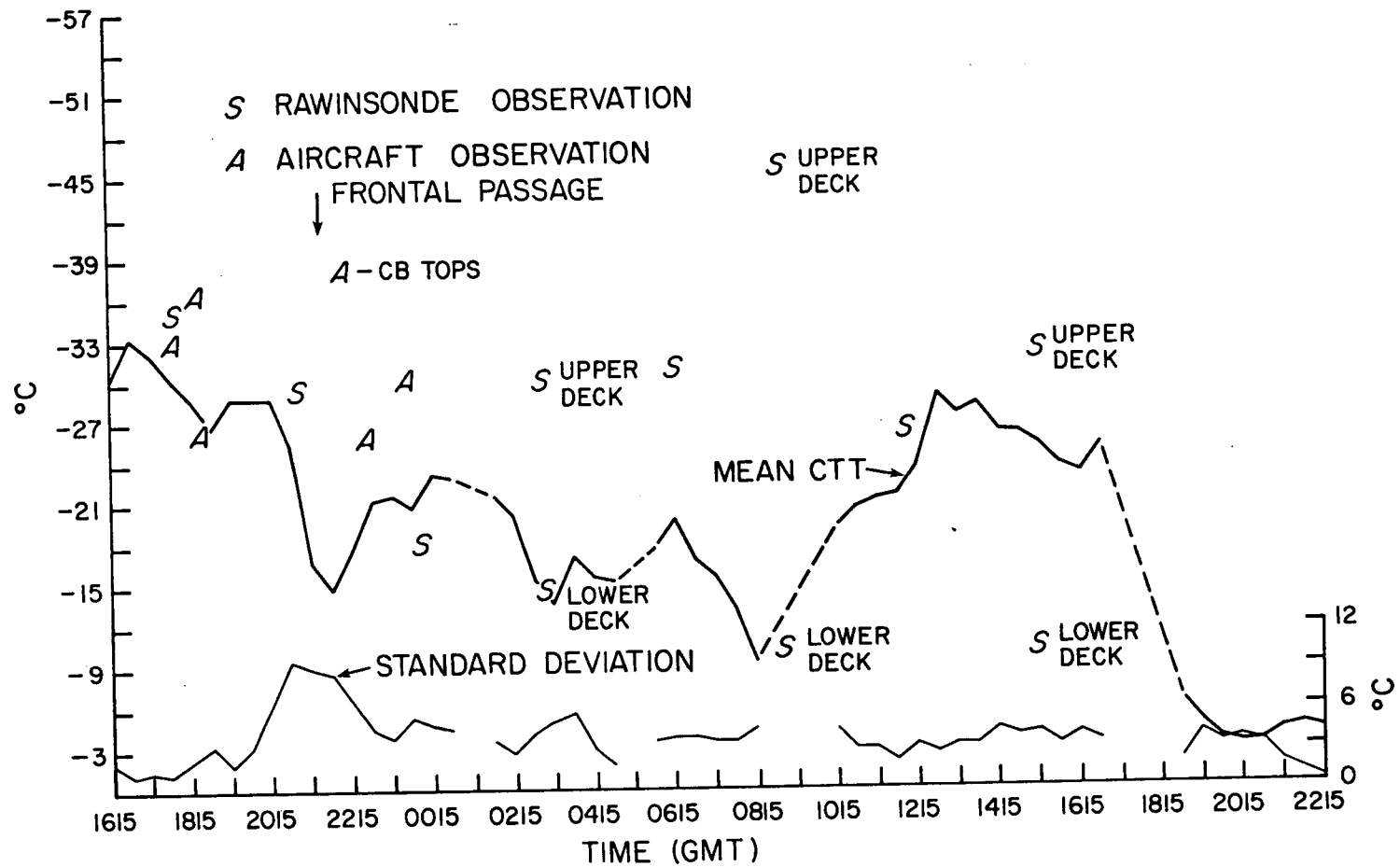


Figure 21. Satellite-observed CTT, 2-3 March 1978.

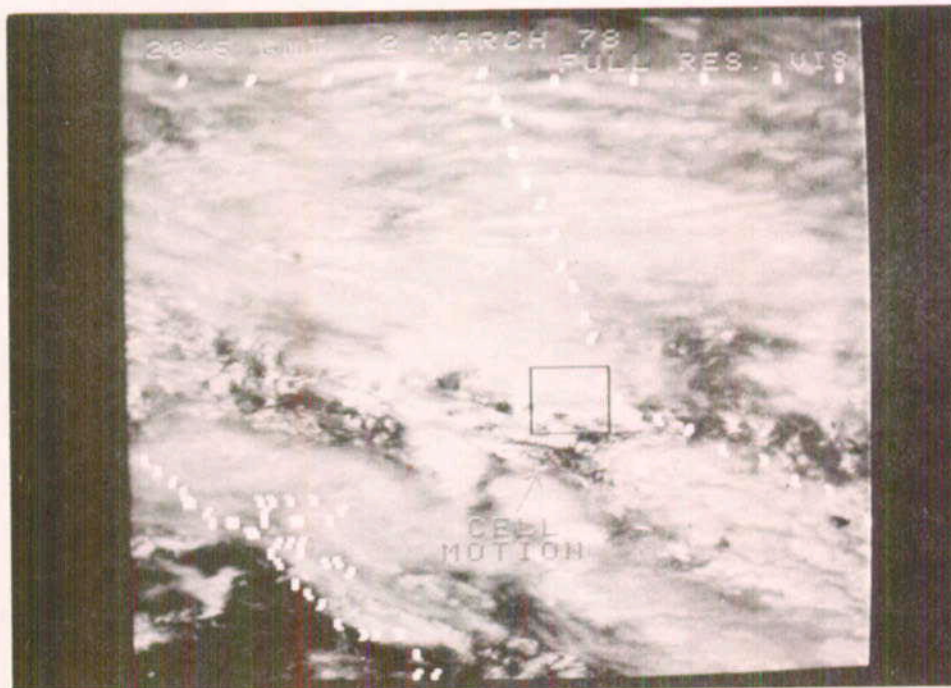
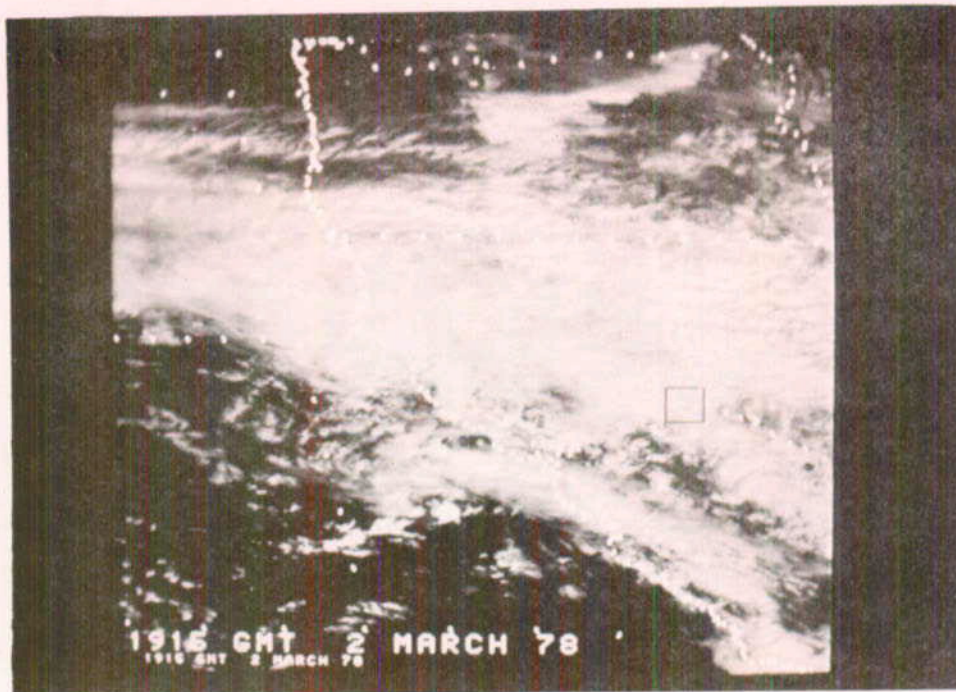


Figure 24. 2045 GMT, 2 March 1978 visible image. Large CB's have developed in the Central Valley within the frontal band.

Speed and direction of movement of the band were determined from the visible images during the time period 1545 to 1915 GMT, while the band was off the coast. Both the center and back edge of the band were tracked, giving nearly identical results. The average movement of the frontal band during this time period was  $211^{\circ}$  at  $17.5 \text{ ms}^{-1}$ . At 1200 GMT, the 50 kPa wind speed and direction at Oakland were  $15.5 \text{ ms}^{-1}$  from  $220^{\circ}$ , while the 70 kPa winds were  $15.5 \text{ ms}^{-1}$  from  $180^{\circ}$ . Figure 23 is the 50 kPa analysis for 1200 GMT. Although the speed of the band was greater than the 50 kPa winds at the coast, the increased height contours' gradient offshore of California implies that the speed of the offshore winds at 50 kPa was faster and closer to the speed of the band.

The orientation of the band was parallel to the surface cold front. Surface analyses of the frontal positions placed the band directly over the front, in the convergence zone. The lower (85-70 kPa) and upper (70-50 kPa) level shear vectors are not related in any obvious fashion to the motion or orientation of the band as found in some previous studies (see section 3-A). It may be that frontal bands are not comparable to imbedded convective bands in this respect, as one would expect a frontal or prefrontal band to always be parallel to the front, independent of the shear.

Cloud top temperature of the convective band decreased from  $-21^{\circ}\text{C}$  to  $-29^{\circ}\text{C}$  as the band moved onshore. This placed the cloud tops around 45 kPa indicating a steering level for the band of just below 50 kPa. Hobbs et al. (1978) found similar results for the orientation and motion of frontal bands off the Washington coast line using mainly radar observations.

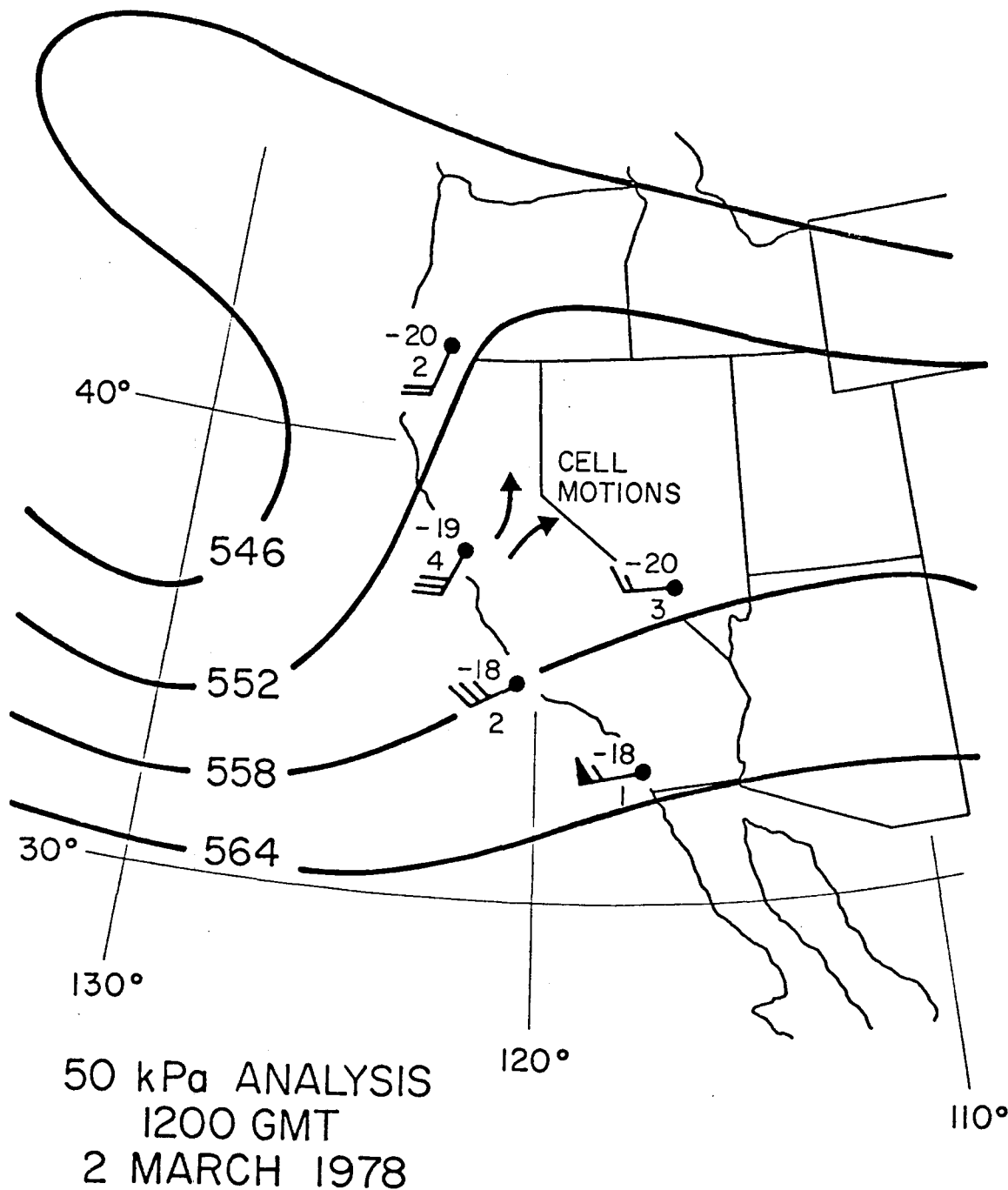


Figure 23. 50 kPa analysis for 1200 GMT, 2 March 1978. 3½ hour movement of individual cells from 1945 to 2315 GMT is plotted. Divergent motion of cells approaching the Sierra and steering by near-50 kPa winds are evident.

Decreasing CTT of the band, from roughly  $-21^{\circ}\text{C}$  to  $-29^{\circ}\text{C}$ , reveals that the convection in the band intensified upon moving onshore. As the band reached the Central Valley, large CB's developed, as seen in the full resolution visible image at 2045 GMT, Figure 24. From 1945 to 2315 GMT individual cells were tracked, as the band moved into the mountains, to determine the influence of the mountain barrier on the motion of cells. The band approached parallel to the Sierra with an interesting phenomena occurring in the movement of the large CB's.

Cells traveled in two different directions depending on their north-south location within this band. South of a line perpendicular to the band and mountains and passing through Lake Tahoe, cells veered off to a more easterly direction and continued to the barrier, where they dissipated. One cell, south of the target area, turned noticeably northeast at the higher mountains and continued to the crest, finally disappearing. It may have possibly followed some topographic feature, such as a mountain valley. Average cell motion, from the valley to the mountains south of the dividing line, was from  $235^{\circ}$  at  $11.6 \text{ ms}^{-1}$ . Cells curved more to the right of this average direction near the Sierra.

North of the dividing line, cells curved to the left as they approached the foothills, until their direction was nearly parallel to the Sierra. Average cell motion on the north side was from  $187^{\circ}$  at  $12.3 \text{ ms}^{-1}$ . Cyclonic curvature of cell trajectories as displayed by these northern cells has previously been observed by Peace (1975) from radar studies during the CENSARE experiment.

Comparing the 50 kPa contours to individual cell trajectories, both plotted on the 1200 GMT chart, Figure 23, both show divergent motion over the Sierra Nevada, with a central axis dividing the cyclonic and

anticyclonic flow described above. The IR images at 2045 and 2145 GMT clearly show the different trajectories of two cells, one north and one south of the dividing line (Figure 25).

CB tops in the onshore band had temperatures varying from  $-36^{\circ}\text{C}$  at 2015 GMT while cells were in the valley to  $-24^{\circ}\text{C}$  at 2245 GMT for cells moving north along the foothills. The 40 kPa and 50 kPa temperatures on the 2100 GMT Sheridan sounding were  $-34^{\circ}\text{C}$  and  $-21^{\circ}\text{C}$ , respectively, with southerly winds dominating from 85 to 30 kPa.

The visible image loop from 1915 to 2315 showed that none of the large CB's entered the target area, hence they can't account for the maximum in precipitation at Donner Summit at 2045 GMT (Figure 26). The large cells seen in Figure 24 either curved away to the north or became unidentifiable upon climbing the mountains to the south. Some small convective elements did enter the target; in fact, two small bands proceeded ahead of the frontal band but were overtaken by it as they slowed along the foothills. The precipitation maximum appears to have been caused by an imbedded cell or group of cells which originated south of the target area on the mountains and moved north-northeast along the west side of the crest, passing over the gage.

Within the satellite target, mean CTT ranged from  $-33^{\circ}\text{C}$  to  $-27^{\circ}\text{C}$  for prefrontal orographic clouds up to 2015 GMT. A sharp increase in CTT took place after 2015, near the time of surface frontal passage. The frontal position as indicated on the 2100 GMT surface analysis, Figure 27, shows that the highest CTT occurred just prior to frontal passage. Clearing occurred in advance of the frontal band, probably due to subsidence surrounding the convective cells. Cirrus cover on the orographic cloud retreated eastward under the influence of the subsidence,

Figure 25.

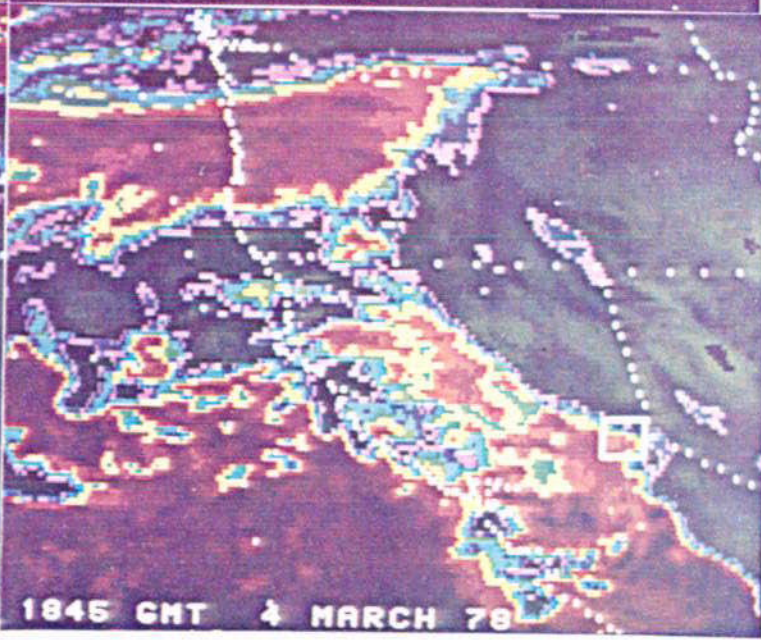
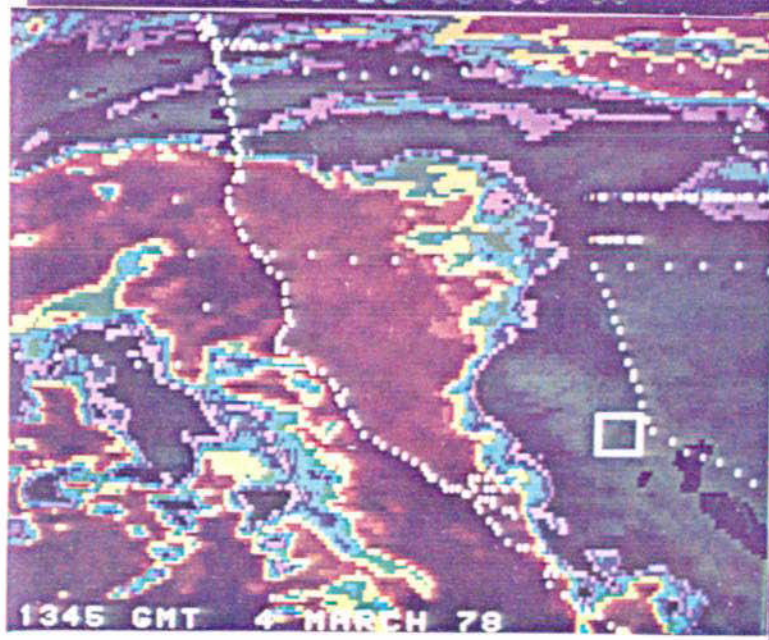
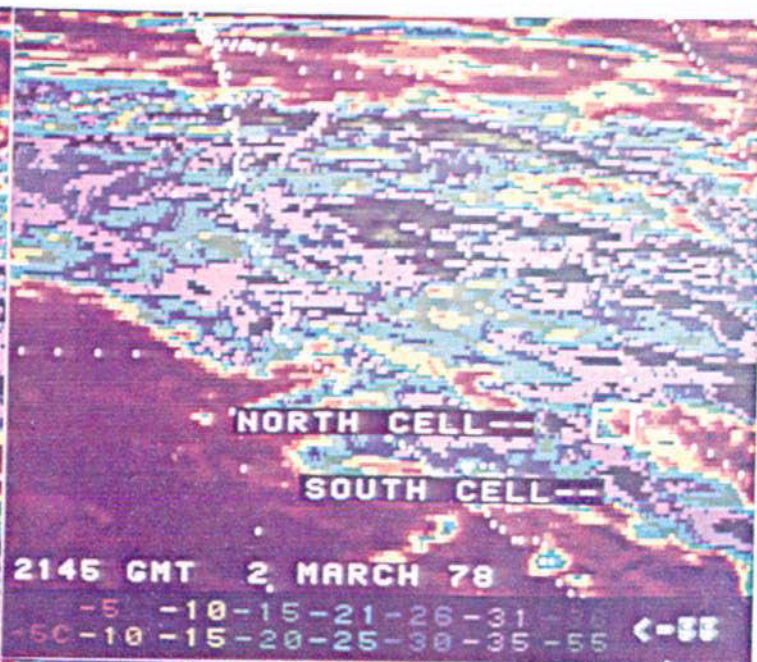
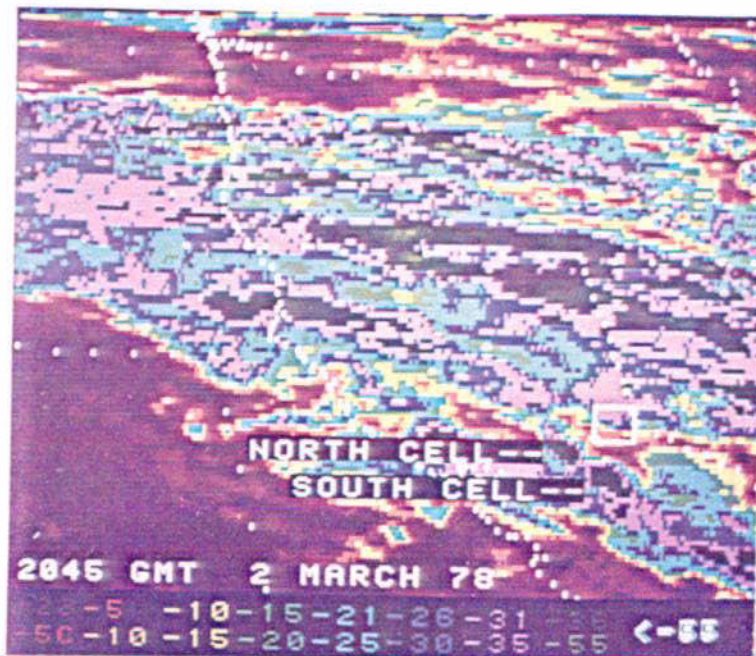
2045 and 2145 GMT, 2 March 1978 IR images. Cells (green) are seen to diverge along the Sierra foothills, avoiding the target area.

Figure 35.

1345 GMT, 4 March 1978 IR image. Massive, cold cloud cover precedes the surface front.

Figure 39.

1845 GMT, 4 March 1978 IR image. Cirrus clears as front progresses to the east. CTT color coding for Figures 35 and 39 same as shown in Figure 25 IR images.



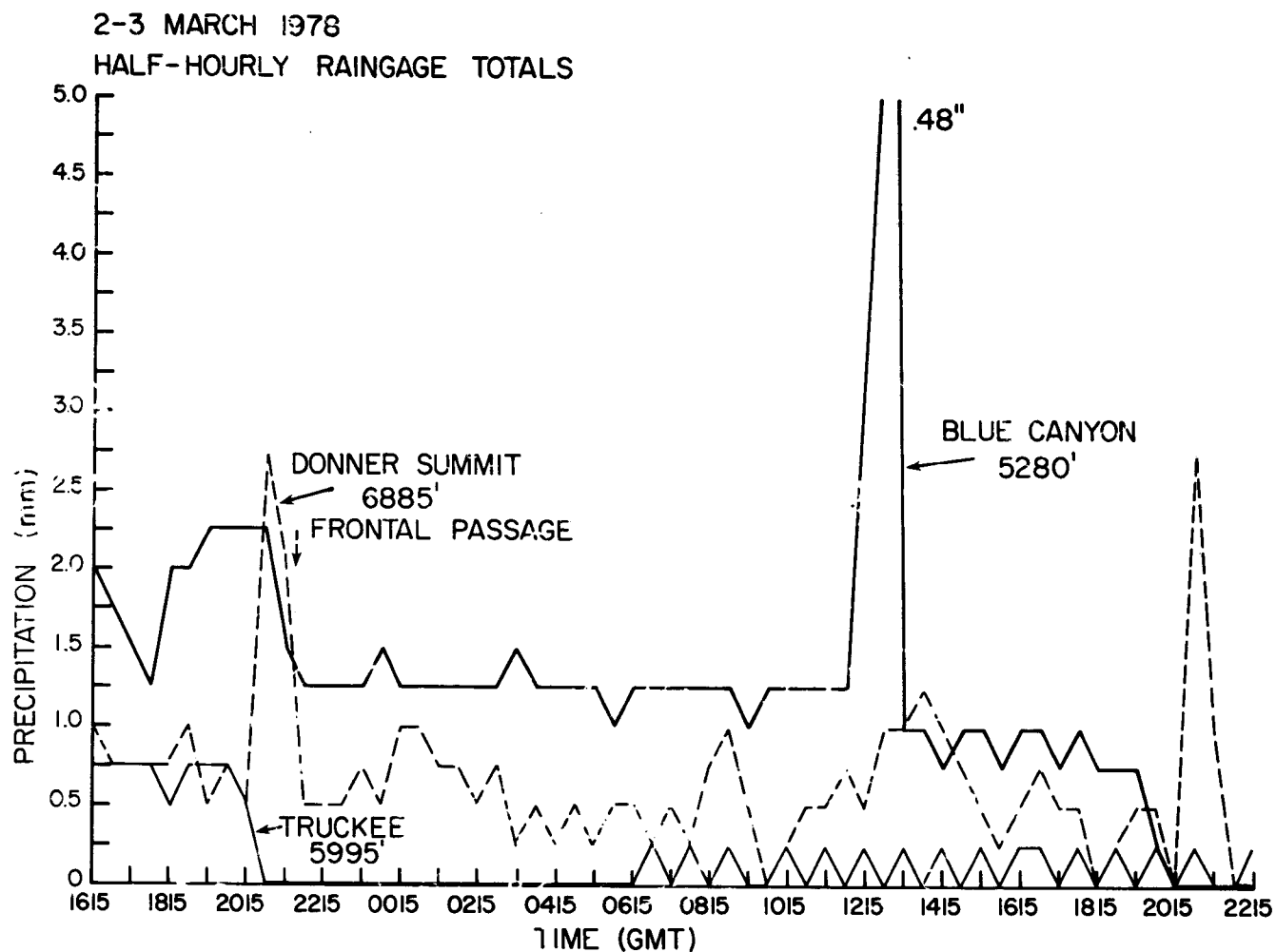


Figure 26. Raingage records for Blue Canyon, Donner Summit and Truckee, 2-3 March 1978.

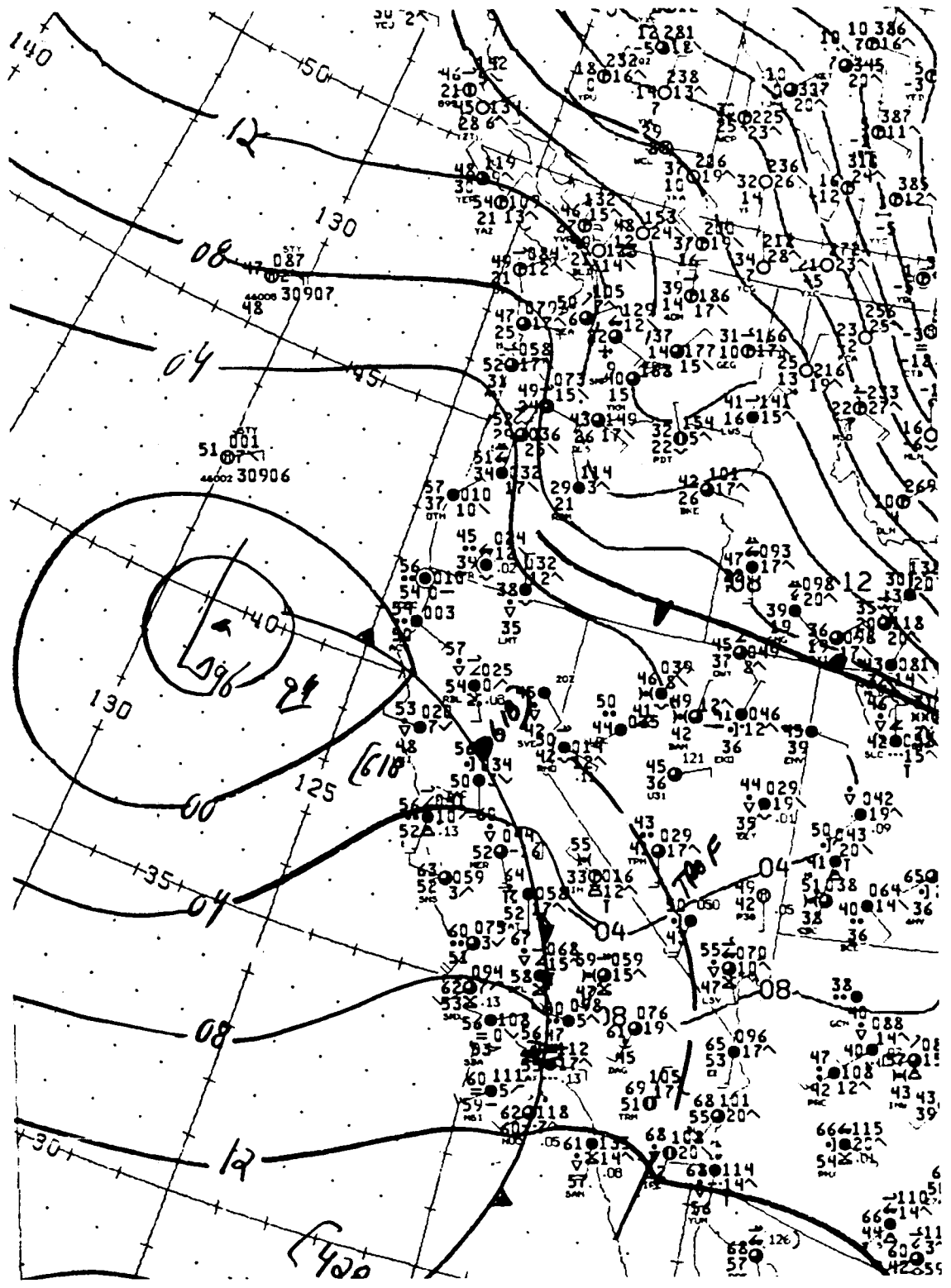


Figure 27. Surface analysis for 2100 GMT, 2 March 1978.

explaining the CTT increase in this case. CTT was lowered after 2145 as the frontal band itself entered the target.

At 2045 GMT, just prior to the frontal passage, precipitation at Truckee ended (Figure 26). This coincides exactly with the warming of the target area cloud tops mentioned above. Donner Pass and Blue Canyon continued to receive moderate amounts of precipitation even during the warming and lowering of the orographic cloud. This effect may be induced by terrain. As opposed to the other two raingage stations, Truckee is on the downwind side of a mountain range. It may be that only with the higher, colder clouds can significant precipitation continue at Truckee as ice crystals at higher altitudes and longer fall times permit falling particles to blow over the crest, reaching the ground on the downwind side of the slope. Presence of a low-level jet (below 80 kPa) at Sheridan seems to relate somewhat to this pattern, although the jet is southerly and below the height of the divide. Precipitation at Reno, which is farther downwind of the Sierra, also ended as CTT increased over the mountains.

## C. 3 March 1978

On March 3, surface analyses did not detect the passage of any fronts through the target area. By 0000 GMT, the axis of the short wave trough was nearly above the target, and the cold core of air aloft with continued moist onshore flow kept the valley and mountains within precipitation. No evidence of any significant convective cells was seen during the late evening hours as revealed by the precipitation records for the mountain stations (Figure 26) and the valley station at Sheridan (Figure 28).

Observations of the IR image loop for 2245, 2 March to 0245 GMT, 3 March revealed that the cloud motion pattern at the Sierra foothills was still divergent, although not as obvious as with the frontal band earlier on 2 March. Three small bands moved from the valley to the target area, dissipating as they reached the higher mountains. CTT of the bands again decreased as convection intensified moving off the Coastal Range into the Central Valley. Coldest tops in the valley ranged from  $-30^{\circ}\text{C}$  to  $-35^{\circ}\text{C}$ . Comparing these temperatures to mean target CTT in Figure 21, individual cells in the valley were as much as  $10^{\circ}\text{C}$  colder, indicating weakening of the large convective cells at the foothills.

A spiral cloud structure, which appears to be associated with the surface low, moved into the coast, slowed and dissipated at 0445 with no apparent effects on the weather there. A slow-moving band was in the target at 0345; a second band passed through the area between 0515 and 0645 GMT and dissipated over the mountains. CTTs of both were above  $-30^{\circ}\text{C}$ , with neither having a visible effect on target precipitation, although Sheridan (Figure 28), the valley station, showed evidence of both in its raingage record.

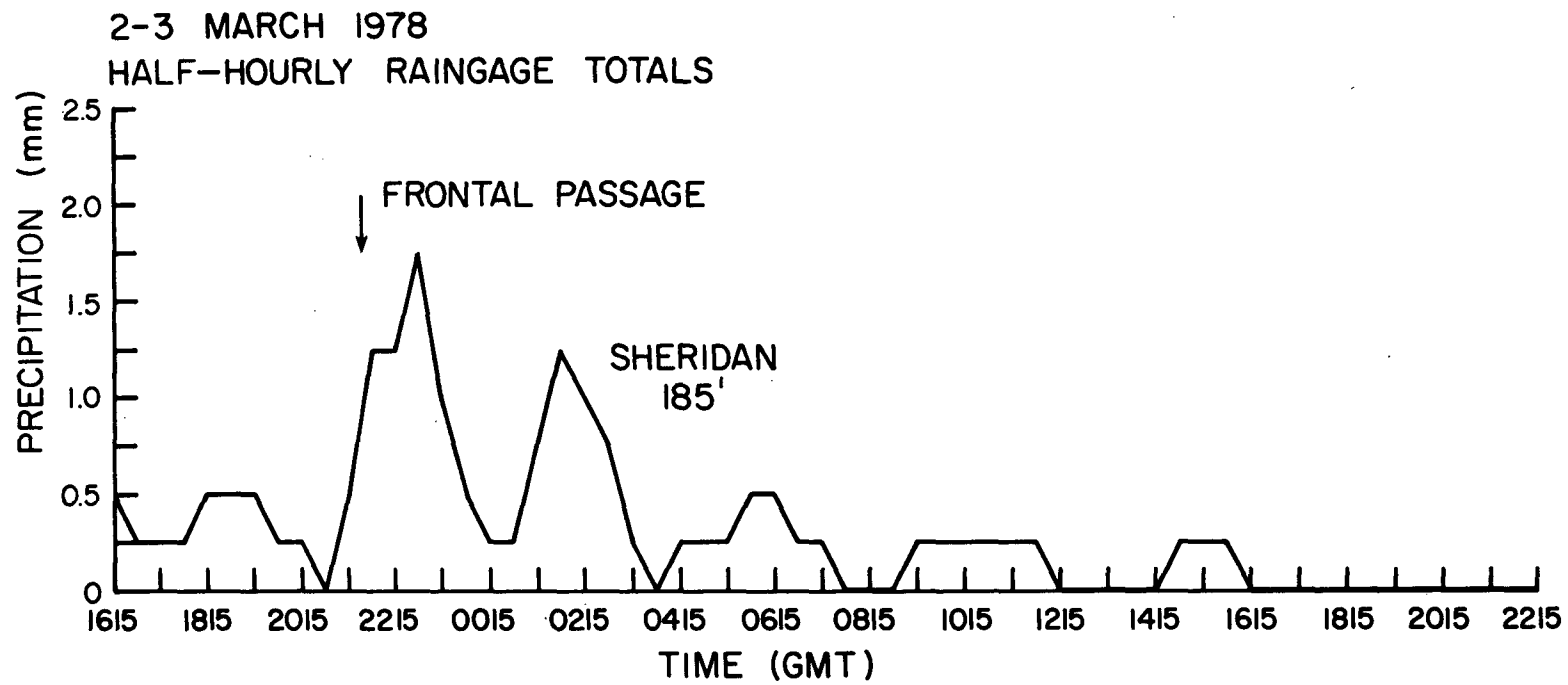


Figure 28. Raingage record for Sheridan, 2-3 March 1978.

During this time, Sheridan soundings indicated the presence of an upper cloud deck not observed by the satellite. The lower clouds' temperature agrees fairly well with the CTT given by the satellite within the target area (Figure 21). The coldest cloud top observed by satellite within at least 100 km was only  $-29^{\circ}\text{C}$ , so a possible explanation may be the lag problem of a wet rawinsonde, because it is unlikely that the sonde could detect a high cloud layer that would be transparent to the satellite's infrared detector.

Two significant bands, one at 1115 and a second stronger band at 1215 GMT, entered the target area almost parallel to the Sierra. Within the target, CTT dropped to  $-29^{\circ}\text{C}$  as the second band entered. Cloud tops were colder in the valley where  $-35^{\circ}\text{C}$  tops were the coldest observed. On the 1200 GMT surface analysis, Red Bluff reported rainshowers and Sacramento reported a thunderstorm. A very vigorous cell dropped 12.2 mm of precipitation at Blue Canyon during the half hour from 1215 to 1245 GMT. The particular cell which generated the extreme precipitation is not obvious in the IR imagery. A wide band of overlying cirrus and cirrus blow-off covered the convection, hiding individual cells from satellite view. Because of the early hour, no visible data were available for detection of convective cells above the cirrus.

A short wave ridge moved over California during the daylight hours of March 3. Cloud tops lowered and major cloudiness cleared during the morning with only marginal precipitation falling by early afternoon. The effect of the Sierran barrier on low level flow became quite apparent as lower and more scattered clouds were able to be seen. Small cumulus clouds formed on the foothills south of the target area, organized in small parallel lines or streets. Cumuli fed up into the

target area along the axis of the semi-stationary streets to the north-northeast. Width of the streets was about 5-6 km and the spacing between streets was usually slightly less than the width. Figure 29 is the full resolution visible image at 2115 GMT containing a typical set of these cloud streets observed in the stable air beneath the short wave ridge.

A sequence of images leading up to this time showed the flow to be south-southwesterly, blocked by the mountains, curving to a southwesterly direction within and to the north of the target area, crossing the mountains which are lower to the north. Larger convective cells fed by the cloud streets formed over the mountains, probably accounting for the maximum in precipitation occurring at Donner Pass at 2045 GMT (Figure 26). The small sizes and short lifetimes of cumuli in the streets made it impossible to determine their exact motion from half-hourly images.

Offshore, a prefrontal band reached the California coastline in the early afternoon, seen on the 2015 GMT visible image, Figure 30. Individual convective elements along the extent of the band were tracked using navigated satellite imagery, from 1815 GMT, 3 March to 0015 GMT, 4 March. The groups of cells tracked in the more northern part of the line remained identifiable for the entire 5 1/2 hours, coming onshore at 2245. Motions of cells throughout the extent and life of the line were found to be identical. Average movement of the three sets of cells was from  $225^{\circ}$  at  $23 \text{ ms}^{-1}$ . By comparison, 700 mb winds at Oakland for 0000 GMT, 4 March were from  $220^{\circ}$  at  $15.4 \text{ ms}^{-1}$  and 500 mb winds were from  $230^{\circ}$  at  $28.3 \text{ ms}^{-1}$ . This is the same result found by tracking frontal band cells on 2 March.

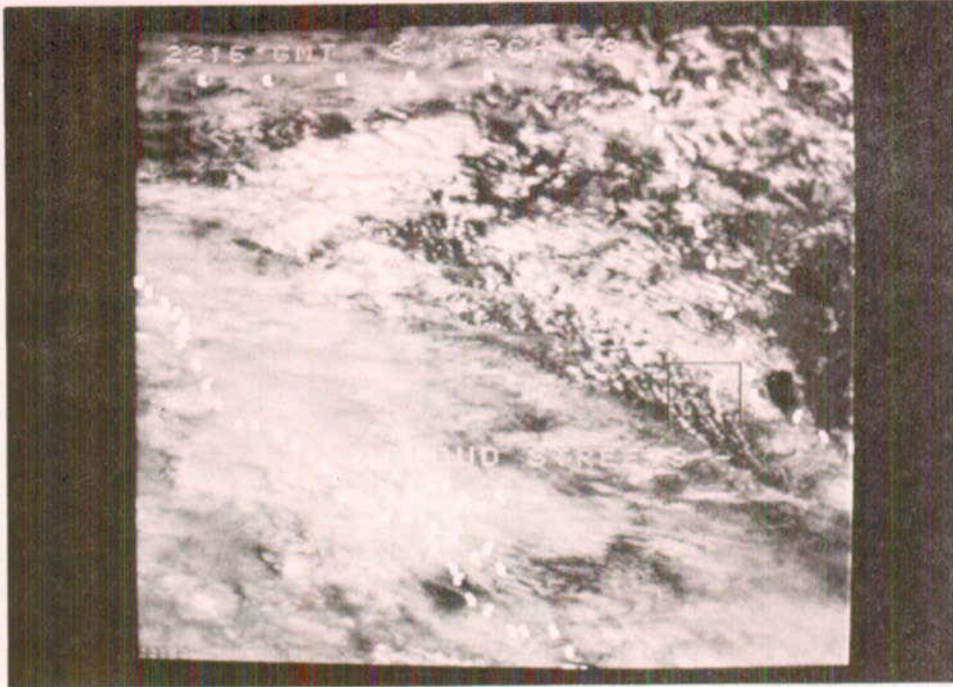


Figure 29. 2215 GMT, 3 March 1978 visible image. Convective cloud streets over the foothills feed up into the target area from the south.



Figure 30. 2015 GMT, 3 March 1978 visible image. Cells in the offshore band were tracked into north central California.

CTT of convective cells tracked range from  $-23^{\circ}\text{C}$  to  $-45^{\circ}\text{C}$  with a modal value of  $-37^{\circ}\text{C}$ . An estimate for the tops of the cells is therefore around 38 kPa. From this information, a steering level for convection in the offshore band can be taken as something below the 50 kPa level.

While offshore, the major effect of the band on the Sierra region was from the cirrus which blew out ahead of the band from the convective tops. Bursts of cirrus passed over the target area around 0000 GMT, 4 March, showing up as colder CTTs in the graph for 3-4 March, Figure 31. Upon crossing the Sierra, this source of moisture led to formation of large wave clouds at intermittent times in the lee of the mountains, such as are seen on the 2345 GMT visible image, Figure 32.

3-4 MARCH 1978

MEAN AND STANDARD DEVIATION OF CTT OVER TARGET AREA

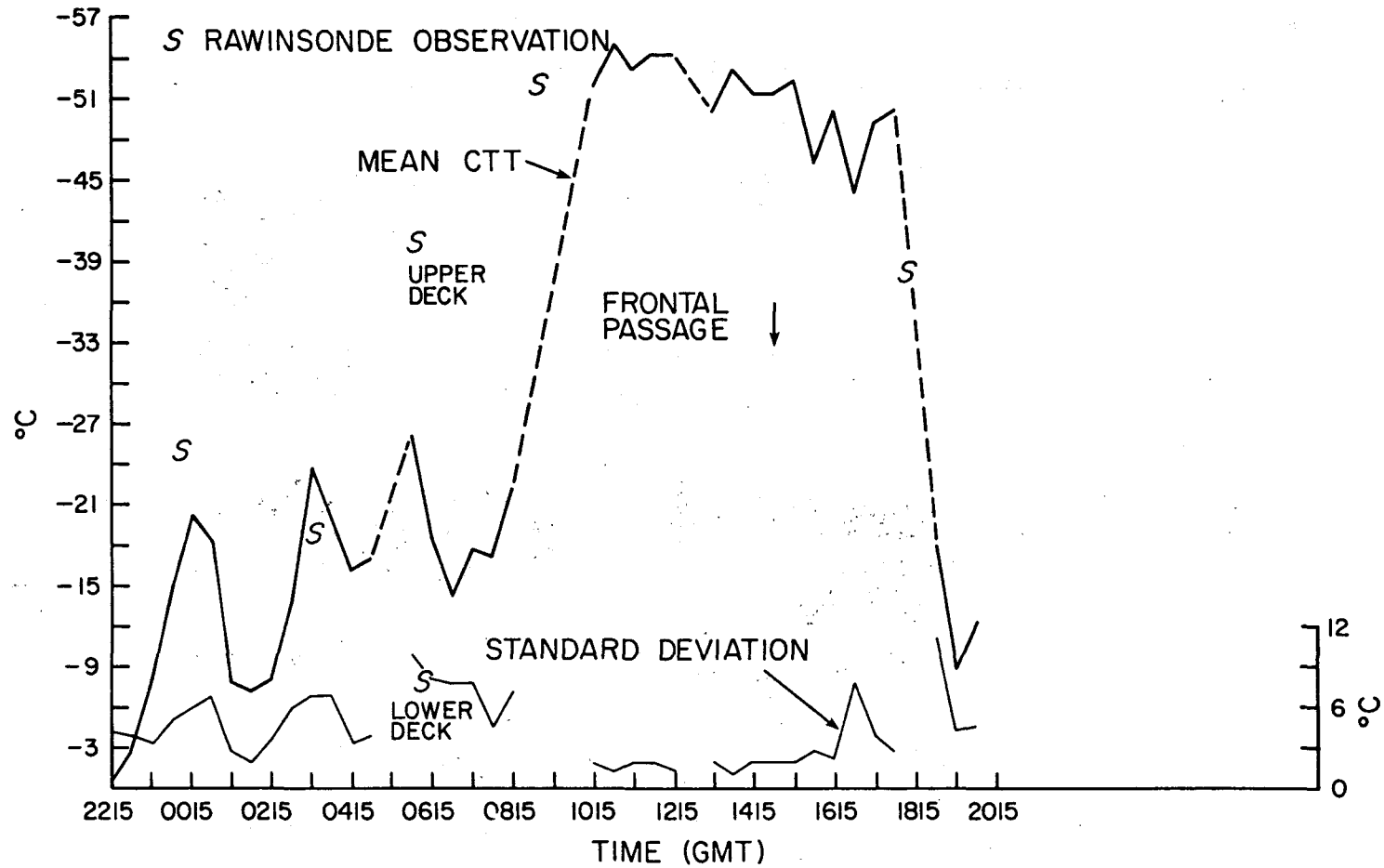


Figure 31. Satellite-observed CTT, 3-4 March 1978.



Figure 32. 2345 GMT, 3 March 1978 visible image.

D. 4 March 1978

By 0315 GMT, the first cells from the prefrontal band reached the Sierra. The anvil of one cell was just within the border of the satellite target area, lowering the mean CTT for this time. As it moved from the Coast Range to the Valley, this cell's CTT decreased from  $-45^{\circ}\text{C}$  to  $-50^{\circ}\text{C}$  near Sacramento, rising again to  $-45^{\circ}\text{C}$  when over the mountains north of the target area, all this within a  $2\frac{1}{2}$  hour period. The massive group of cells in Figure 32, 200 km off the coast west-southwest of San Francisco, split into two parts, the northern part going north-northeast up the coast into north central California. Cells of the southern part stayed on a steady northeast course, passing over the northwest half of the target area at 0545 GMT, dropping 3.3 mm of precipitation at Blue Canyon during the preceding half hour (Figure 33). Contrary to cells observed in bands on the previous days and other cells within this band, this group intensified upon moving from the valley up the foothills and did not curve cyclonically upon encountering the mountain barrier. In contrast to the southerly 50 and 70 kPa winds on 2 March when cells curved cyclonically, the winds on this day were from  $220^{\circ}$  and faster at both levels on the 0600 GMT, 4 March sounding at Sheridan. CTT of these cells lowered from  $-45^{\circ}\text{C}$  to  $-53^{\circ}\text{C}$  as they neared the crest, warming again at the California-Nevada border. The cell or group of cells travelled along a straight line through the mountains and into northwest Nevada.

Precipitation records from Sheridan (Figure 34) indicated the passing of cells and bands described above better than records from the mountain stations. The orographic precipitation effects seemed to smooth out or cover up the band passages in some cases. Cells were

3-4 MARCH 1978  
HALF-HOURLY RAINGAGE TOTALS

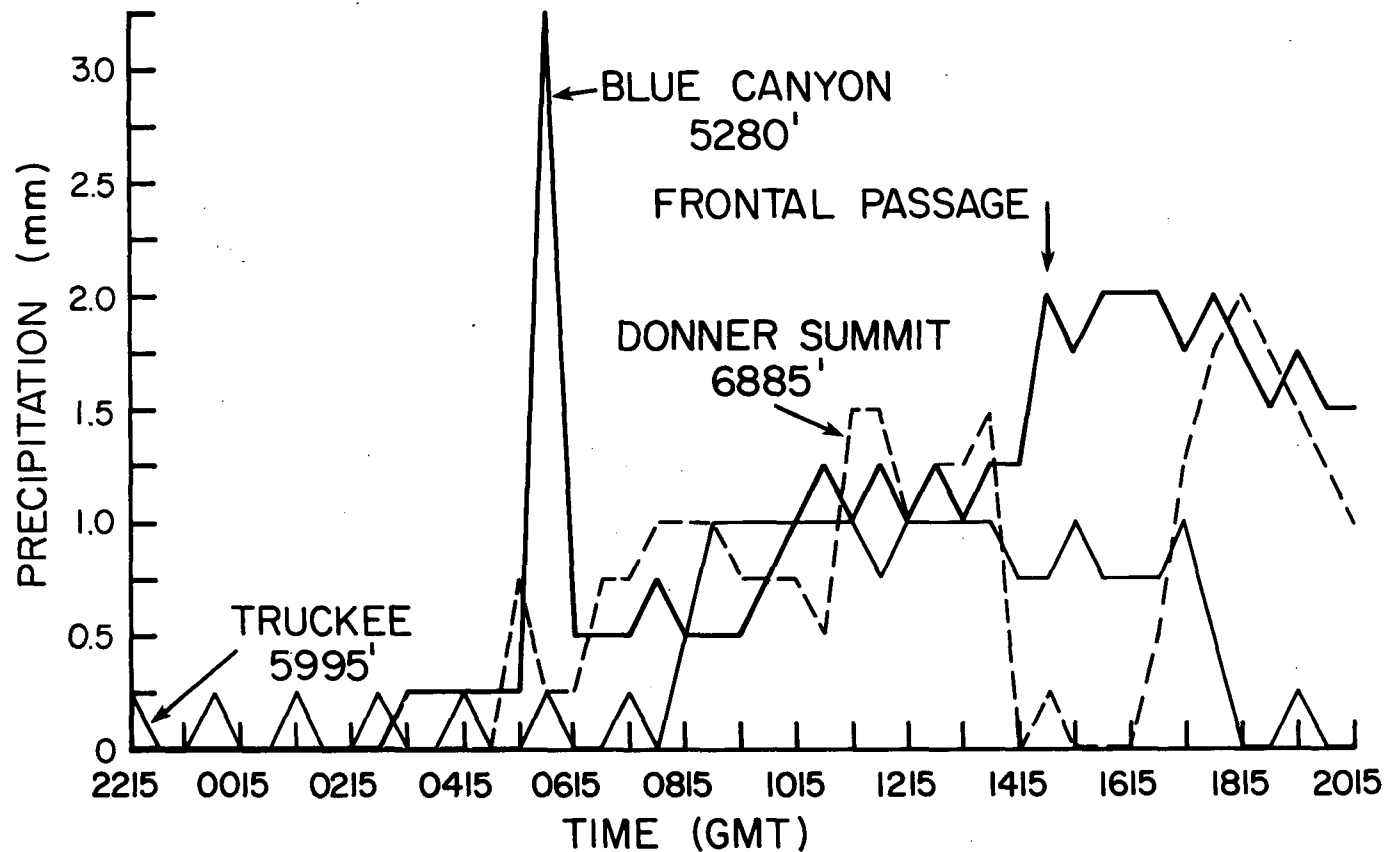


Figure 33. Raingage records for Blue Canyon, Donner Summit and Truckee, 3-4 March 1978.

3-4 MARCH 1978  
HALF-HOURLY RAINGAGE TOTALS

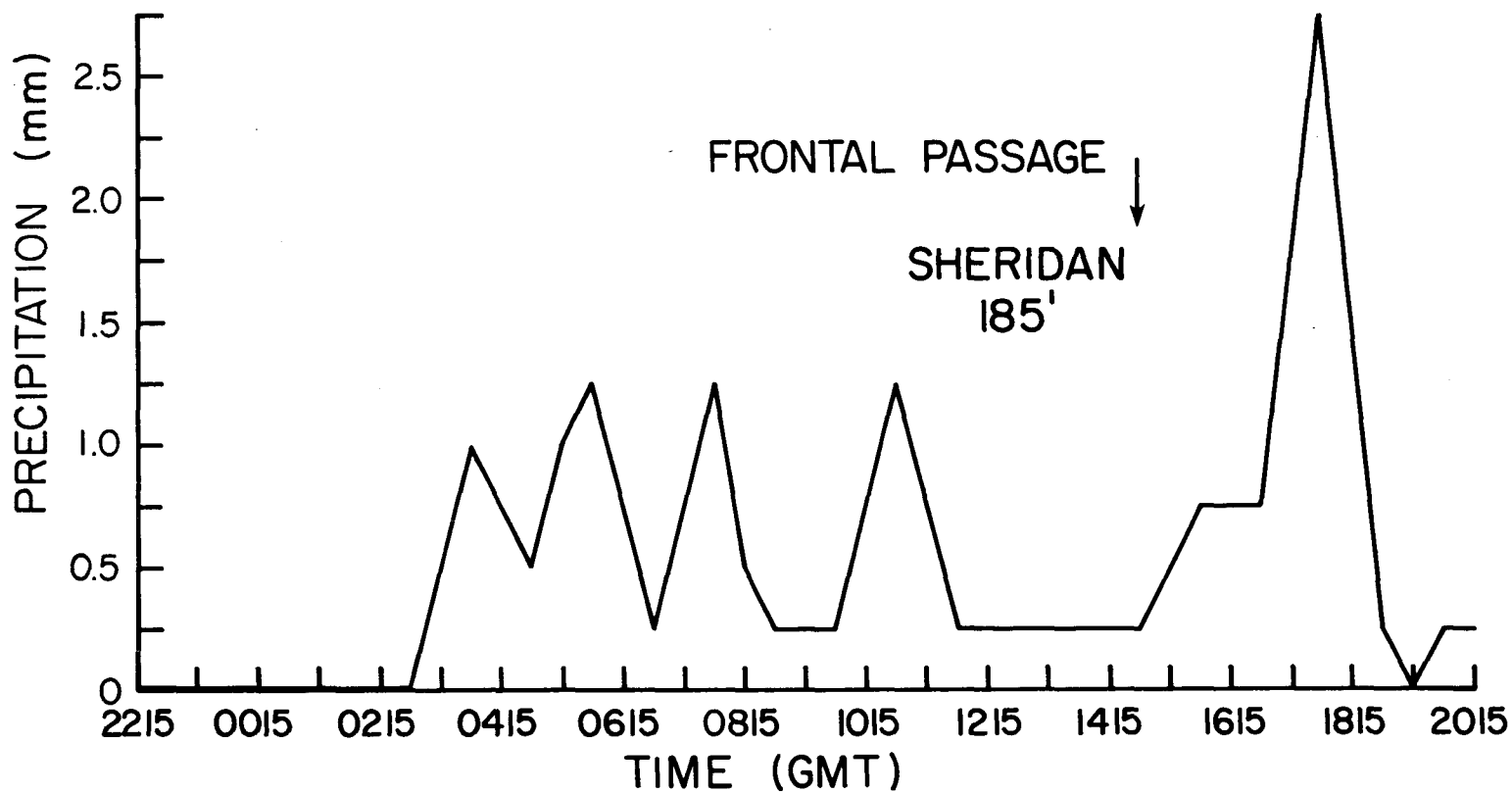


Figure 34. Raingage record for Sheridan, 3-4 March 1978.

generally observed to intensify in the Central Valley and dissipate over the mountains, making them easier to identify in valley precipitation records. A notable exception is the 0545 GMT precipitation at Blue Canyon from the cell which intensified over the foothills.

Rawinsonde cloud top from 0600 GMT at Sheridan seems to bear no relation to the satellite observed CTT on Figure 31. However, the precipitation record and the satellite images showed that a convective band was present at this time. The sonde had encountered a cirrus or moist layer in the band whose coldest cell top, which filled one corner of the satellite target, was about  $-53^{\circ}\text{C}$ . This lowered the mean CTT in the area and increased the standard deviation of CTT. On the other hand, low average CTT and standard deviation indicate wide frontal bands that have large areas of overlying cirrus, very smooth and homogenous in general.

Such a cirrus-covered cloud mass south and west of the Sierra moved to the east-northeast over the project area in advance of the approaching short wave at 50 kPa and the surface cold front. Starting at 0815 GMT, CTT over the target area fell dramatically, to  $-52^{\circ}\text{C}$  at 1015 GMT (Figure 31). Significant precipitation had been falling at Blue Canyon and Donner Pass since 0515 when the first convective cells hit the area. Not until the large cirrus mass began to cover the target at 0815 did precipitation increase at Truckee (Figure 33).

No high-level cirrus cap of great extent was present during the nearly identical frontal passage on 2 March. The difference between the two days was in the upper atmospheric circulations at the cirrus level. On 2 March, the 20 kPa flow was zonal and straight westerly. By 4 March, a trough had developed and was off the coast at 1200 GMT, putting

California under southwest to southerly winds at all upper levels, giving rise to the presence of cirrus. The 1345 GMT IR image (Figure 35) reveals some of the extent of upper cloudiness accompanying the cold front.

Surface analysis placed the cold front in the target at 1500 GMT. Precipitation ended at Donner Pass from 1345 until 1615, while Blue Canyon and Truckee showed no changes in precipitation intensity (Figure 33). The reason for the lack of precipitation at Donner Pass was not evident, due to screening of the satellite by the overlying cirrus and extensive range from the Sheridan radar.

The trailing edge of the cirrus shield did not move east with the cold front as on other days, if the analysis of the frontal position at the surface is correct (Figure 36). Frontal positions are quite difficult to determine in California because of the stable pool of air in the Central Valley. Often, no significant wind shift, temperature or pressure changes occur at the surface with the front, as the cold air is initially aloft moving across the valley (Marwitz et al., 1978). With this in mind, no conclusions will be drawn here as to whether the cirrus extended far westward over the front or was retreating with the front.

Along its trailing edge, the cirrus was detached from the lower clouds, which is the impression one gets from the 1745 GMT visible image, Figure 37. Verification of the satellite observation is from the 1800 GMT Sheridan sounding and more dramatically, from airborne photographs taken around the same time. Figure 38 is the view to the south from a point west of the target at 1830 GMT from the vantage point of a project airplane. It clearly shows the western edge of the cirrus with the convective precipitating clouds well below it. IR imagery at 1845 GMT

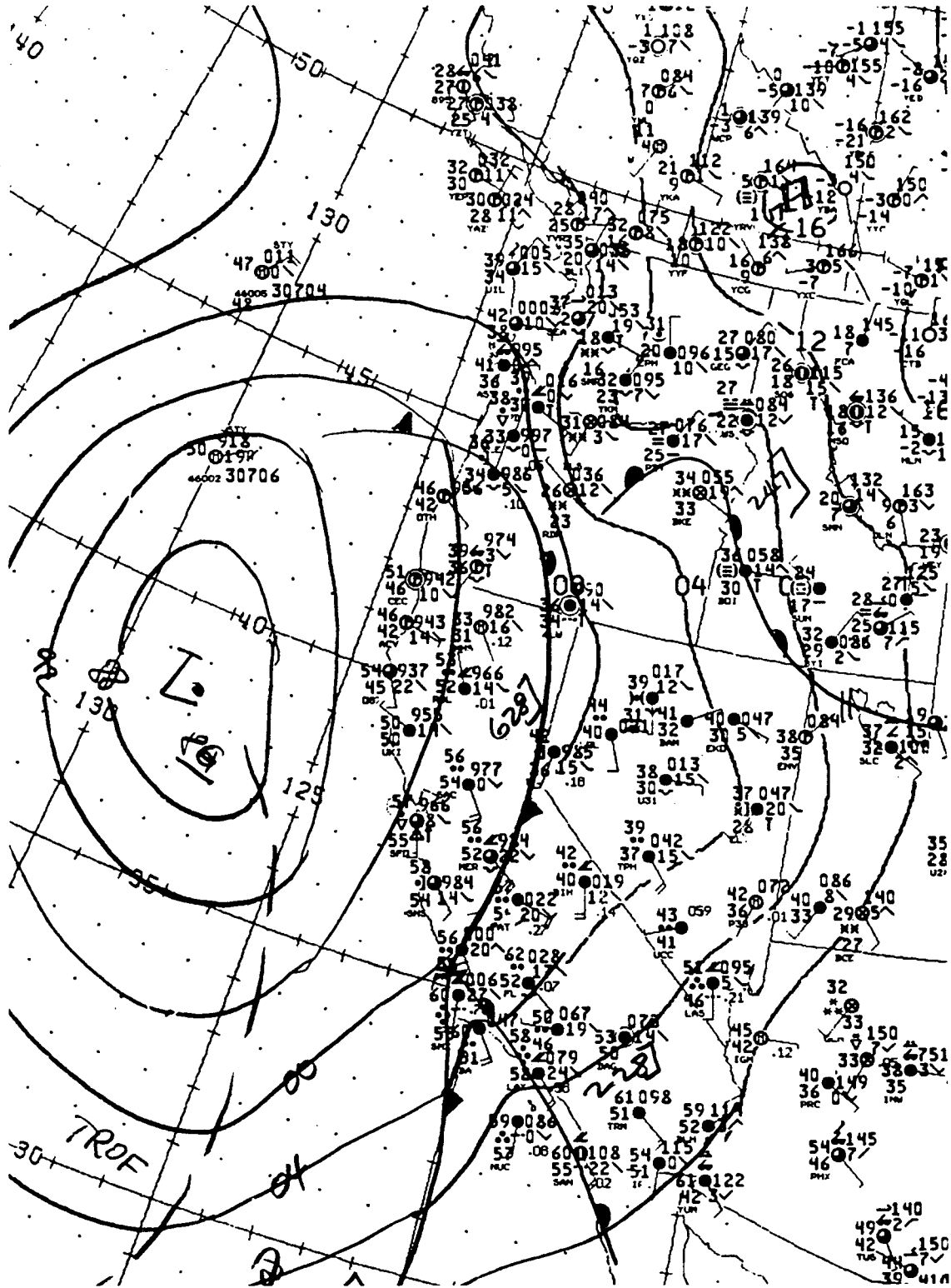


Figure 36. Surface analysis for 1500 GMT, 4 March 1978.

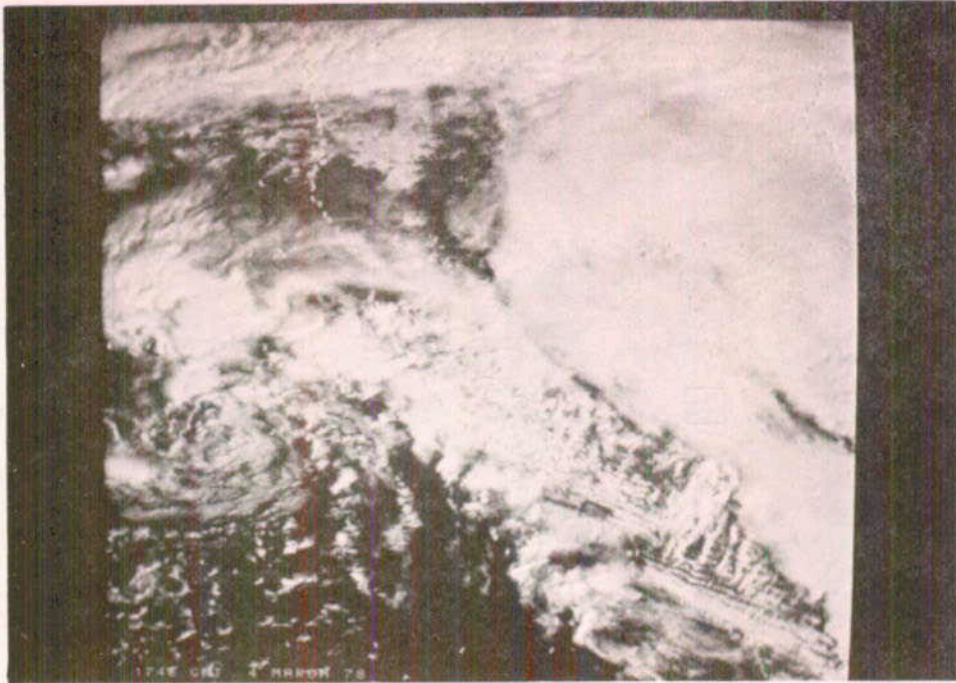


Figure 37. 1745 GMT, 4 March 1978 visible image. Cirrus ahead of the front casts shadows on lower clouds. Time-lapse imagery showed that the cloud streets extended northeast from the Coast Range, criss-crossing lee wave clouds.



Figure 38. Cloud photo from aircraft at 1830 GMT, 4 March 1978. Western edge of the cirrus is seen above the lower clouds. View is to the south. Aero Systems aircraft; photo by J. Moore.

(Figure 39) shows the cold cirrus (as low as  $-55^{\circ}\text{C}$ ) departing the target area, exposing the convective orographic cloud below. CTT of the postfrontal orographic cloud averaged around  $-10^{\circ}\text{C}$ . The convective character of these clouds is seen in the 1915 GMT visible image from the satellite, Figure 40, and for comparison, Figure 41 is a view to the west of the target from the aircraft at 1900 GMT.

At about the time when the cirrus cap moved east of the target, precipitation almost completely ceased at Truckee, yet continued at Donner Summit and even increased to 4.6 mm per hour after 2145 GMT at Blue Canyon. Obviously, the post-frontal orographic cloud is capable of producing significant precipitation on the windward slopes with continued moist flow.

Returning to Figure 37, it appears that low-level moisture was being channeled through the Coast Range south of San Francisco. Cloud streets fed up into the Sierra, criss-crossing wave clouds in the lee of the Coast Range. The role which these cloud streets play in concentrating precipitation in a particular place or enhancing overall rain and snow amounts is not clear.



Figure 40. 1915 GMT, 4 March 1978 visible image. Convective orographic cloud remains after front has passed.



Figure 41. Cloud photo from aircraft at 1857 GMT, 4 March 1978. View is to the west of the target area. Compare to the satellite image in Fig. 40. Aero Systems aircraft; photo by J. Moore.

### E. Summary of the 2-3-4 March 1978 Storm

The synoptic differences between the 2-3-4 March 1978 storm and previous storms studied in this paper were reflected in the cloud types observed from the satellite. The predominance of mesoscale convective bands and large convective cells was unique to this storm. A total of thirteen distinct convective bands were detected in the visible and infrared satellite imagery as having entered the satellite target area. Two frontal bands which extended 800 km or more in length were each preceded by two prefrontal bands. The two prefrontal bands on 2 March were generated just in advance of the frontal band and were completely insignificant in effect. Prefrontal bands on 4 March passed the target 9 and 11 hours ahead of the front, appearing in both rain gauge and CTT records. Five post-frontal bands, of which only two had visible effects on CTT and precipitation, entered the target within 7 hours of the frontal passage on 2 March. Two significant bands associated with a secondary cold front or surface trough followed 13-14 hours after the primary cold front on 2 March. A cell in the second band accounted for the most extreme precipitation event detected in the entire storm.

All bands were oriented parallel to the surface cold fronts and due to the location of low pressure centers northwest of the project area bands were parallel to the Sierra when they encountered it. Individual cells in the bands moved with the winds somewhat below the 50 kPa level until they reached the Sierra foothills. Effects of the Coast Range on cell motion were negligible. Cell trajectories curved cyclonically at the western foothills of the Sierra when 50 kPa map contours indicated a southerly wind component relative to the Sierra and winds of the Sheridan sounding were southerly up through the level of

the cell tops. In the situation on 2 March, 50 kPa winds at Sheridan were directly from the south when the height contours indicated a south-westerly wind direction over and upwind of the target area. Thus the steering level winds showed the same cyclonic curvature at the foothills as the cell trajectories. This curvature kept large CB's from entering the target area on 2 March when cells directly approaching the target area went north along the foothills and those further south followed the flow there into the Sierra. Later in the storm when steering level winds at Sheridan were from  $220^{\circ}$  or more, cells did not turn to the left at the foothills but continued along a straight line into the Sierra.

Decreasing cloud top temperatures of cells entering the Central Valley indicate that cell growth occurred there. Dissipation took place along the foothills and higher mountains where tops of cells became warmer. An exception was the cell in the target at 0545 GMT, 4 March whose CTT decreased nearly  $10^{\circ}\text{C}$  as it approached the Sierra crest. Cells in the valley had CTTs ranging from  $-30^{\circ}\text{C}$  to  $-53^{\circ}\text{C}$ , averaging about  $-37^{\circ}\text{C}$ . Coldest tops were with cells in the prefrontal band on 4 March.

Precipitation from convective bands was much more evident in the raingage records from Sheridan in the valley than in those from Blue Canyon, Donner Summit or Truckee. Dissipation of bands and cells and curvature of cell trajectories away from the target area, as well as orographic lifting leading to more continuous precipitation over the mountains account for this observed effect.

Most precipitation at Truckee and Reno fell while cold clouds covered the Sierra orographic cloud, with target area CTT of  $-30^{\circ}\text{C}$  or less. It appears that in orographic clouds with tops warmer than this,

precipitation tends to be concentrated on the upwind slopes, due to the shorter fall times of precipitation particles in the cloud of less vertical extent allowing the particles to reach the surface before being carried over the crest. Both Truckee and Reno are downwind of the main Sierra crest where dissipation of a shallower orographic cloud would take place. With a deeper orographic cloud or with cirrus covering the orographic cloud, precipitation particles could originate at higher altitudes and be carried over the crest to be deposited on the lee slopes. One would also expect a different crystal type, which could have a slower fall speed and reach the surface beyond the crest more often, to precipitate from a cloud with a lower CTT. No sharp peaks in precipitation rate occur in the records from Truckee, implying a decrease or lack of convective activity on the lee slopes of the Sierra.

Cloud tops over the target became warmer and lower and precipitation generally decreased following the frontal passages. The decrease in precipitation was not as pronounced as in previous case studies due to nearly continuous moist southwesterly flow on 2-3-4 March. A large cirrus shield was not present with the frontal bands until upper atmospheric (20-30 kPa) troughing and southwesterly flow at these levels developed off the west coast on 4 March. Cirrus retreated eastward near or behind the passing cold front on 4 March exposing a vigorous convective orographic cloud over the Sierra.

The channeling of low-level airflow by the Sierra was seen in the motion of small cumulus clouds on 3 March. Under the short wave ridge cloud streets formed along the Sierra foothills, oriented north-south. Individual cumuli moved north in the streets, feeding up into the mountains within the target area. North of the target where the Sierra

crest is lower, cloud streets and trajectories curved to the right and proceeded to the northeast, crossing the mountains. The presence of a temperature inversion near mountaintop level enhanced the blocking effect of the Sierra.

## 5.0 CONCLUSIONS

Five Sierra storms of the winter seasons of 1976-77 and 1977-78 have been studied in detail using time-continuous digital satellite imagery. Use of the display capabilities of the CSU ADVISAR revealed some characteristics of these storms which otherwise would have been impossible to obtain. Although each storm was unique due to differing combinations of synoptic conditions, a general pattern emerges to enable "typical" storm sequences to be defined. On the basis of satellite-observed storm cloud characteristics, storms have been grouped into three types. Storm Type 1 generally lacks cirrus cover over the frontal band or the orographic cloud. Convective bands are rare and are imbedded in the orographic cloud if they occur. Storms of Type 2 have extensive cirrus cover over and ahead of the frontal band, cover a larger area and produce more total precipitation than Type 1 storms. Cirrus cover obscures satellite observations of any convective bands. Type 3 storms are of long duration, being associated with semi-stationary low pressure centers off the west coast of the U.S. Many synoptic and meso-scale convective bands and large convective cells occur in this type of storm. Storm sequences and observed structure for each storm type as a function of time from frontal passage at the target area are summarized below.

## STORM TYPE 1

Synoptic Characteristics: Single cold front associated with a short wave trough at 50 and 70 kPa. Nearly zonal winds at 20 and 30 kPa in eastern Pacific.

Case Study Examples: 9 March 1977, 14-15 December 1977.

Period I: 7-12 hours before frontal passage at target.

1. Moisture increases at middle and upper levels.
2. Orographic cloud forms over the Sierra, stable, non-convective, CTT -5 to -10°C.
3. Weak upslope wind component, winds south-southwest at 7-10 m/s at 85 and 70 kPa at Sheridan.
4. Precipitation rate 1-3 mm/hr on upwind mountain slopes.
5. May or may not be an overlying cirrus layer.
6. No cloud bands observed by satellite.

Period II: 2-7 hours before frontal passage at target.

1. Moisture and instability increase from surface to 70 kPa.
2. Orographic cloud over Sierra has CTT of -10 to -20°C and appears to be stratiform and glaciated, lacking convection.
3. Strong upslope wind component and low-level jet may accompany a pre-frontal trough and cloud mass, CTT < -40°C, precipitation rate > 10 mm/hr over mountains (14-15 December case only).
4. No layering of clouds evident on soundings, satellite observes CTT of precipitating cloud.
5. No cloud bands observed by satellite.
6. About 50% of storm's precipitation over the Sierra occurs during this period.

Period III: 0-2 hours before frontal passage at target.

1. Frontal cloud band within target, CTT -25 to -35°C, merges with Sierra orographic cloud.
2. Convection begins within the orographic cloud as cold air intrudes at middle and lower levels.
3. Short (~ 1 hr) interval of intense precipitation, 7-10 mm/hr over the mountains.
4. Winds nearly perpendicular to barrier, 15-20 m/s at 85 kPa.
5. Lowest CTT and highest precipitation rate over target area of the entire storm occurs in the hour before frontal passage, cloud heights and precipitation rates begin to decrease sharply after this time.
6. No layering of clouds or overlying cirrus.

Period IV: After frontal passage through target area.

1. Imbedded convective cells and narrow convective bands occur within the unstable post-frontal orographic cloud.
2. Large post-frontal convective band may occur due to lagging trough at middle levels and give a secondary precipitation maximum 1-2 hours after frontal band passes.
3. CTT of orographic cloud rises to  $\sim -15^{\circ}\text{C}$  within 2 hours after front.
4. Precipitation rate 1-3 mm/hr for up to 4 hours after front.
5. Low ice crystal concentration and high liquid water content-- up to  $4 \text{ gm/m}^3$  within convection.

## STORM TYPE 2

Synoptic Characteristics: Single cold front associated with a short wave trough at 50 and 70 kPa. Trough at 20 and 30 kPa off west coast of U.S., southwesterly flow over the Sierra at these levels.

Case Study Examples: 17-18 December 1977, 8-9 February 1978

Period I: 7-12 hours before frontal passage at target.

1. Moisture increases at middle and upper levels, warming near 70 kPa.
2. Orographic cloud over the Sierra obscured by widespread cirrus.
3. Orographic wind component depends on 70 kPa. height gradient.
4. Light rain in Central Valley westward to California coast.
5. Precipitation rate 1-2 mm/hr over the Sierra.
6. No cloud bands observed by satellite.

Period II: 2-7 hours before frontal passage at target.

1. Moisture increases at low and middle levels, stability may increase or remain the same.
2. Orographic wind component increases, 85 kPa wind 20-25 m/s from the southwest.
3. Upper and lower cloud layers separated by a 1-1.5 km gap on Sheridan soundings. CTT of lower cloud layer  $\sim -15^{\circ}\text{C}$  from soundings, of upper clouds  $< -40^{\circ}\text{C}$  from satellite observations. Cirrus moves parallel to frontal band.
4. Moderate to heavy rain falling from Sierra foothills westward to the coast.
5. Precipitation rate 3-8 mm/hr over the Sierra.
6. About 60% of storm's precipitation over the Sierra falls during this period. Precipitation rate peaks 2-3 hours before front passes target.

Period III: 0-2 hours before frontal passage at target.

1. Precipitation rates drop sharply to  $\sim 1$  mm/hr over the target at frontal passage.
2. Low-level instability increases as cold air intrudes at middle levels. Moisture is greatly reduced at low and middle levels.
3. Cirrus covers target area, CTT lowest ( $-50^{\circ}\text{C}$ ) 1 hr before frontal passage. Obscures satellite observations.
4. Light orographic wind component,  $< 10$  m/s.

Period IV: After frontal passage through target area.

1. Mid-level drying continues.
2. Cirrus covers the Sierra for up to 2 hours after front passes.

3. Precipitation rate  $< 1$  mm/hr over the Sierra, lasts  $\sim 4$  hrs.
4. Very light winds below mountain top level.

## STORM TYPE 3

Synoptic Characteristics: Stationary closed low off West Coast of U.S. from surface to 50 kPa. Moist southwesterly flow into the Sierra throughout these levels. More than one cold front and short wave trough may be generated and pass the target area. Highly convective frontal and mesoscale cloud bands containing large individual cumulonimbi form offshore and move into the Sierra.

Case Study Example: 2-3-4 March 1978

Period I: 7-12 hours before frontal passage at target.

1. Moisture is continuous, near saturation from sfc to  $\sim 60$  kPa.
2. Convective orographic cloud over Sierra, CTT  $-15$  to  $-20^{\circ}\text{C}$ .
3. Scattered and intermittent cirrus present.
4. South to southwest winds at Sheridan, sfc to 50 kPa, weak upslope component.
5. Light rain in Central Valley and along coast.
6. Prefrontal convective bands observed, parallel to the front, form offshore and move into the Sierra.
7. Precipitation  $\sim 1$  mm/hr over target except when band passes over.

Period II. 2-7 hours before frontal passage at target.

1. Vertical profiles nearly unchanged.
2. Orographically-induced precipitation 2-4 mm/hr over target, up to 7 mm/hr when pre-frontal convective bands pass.
3. Cirrus deck moves over Sierra if 30 kPa trough approaches with front. CTT of cirrus  $< -50^{\circ}\text{C}$ , of convective orographic cloud  $-30^{\circ}\text{C}$ .

Period III: 0-2 hours before frontal passage at target.

1. Mid-level moisture reduced by subsidence ahead of convective frontal band.
2. Little change in orographically-induced precipitation rate.
3. Cells in frontal convective band grow rapidly in Central Valley, their CTT's near  $-40^{\circ}\text{C}$ .
4. CTT of convective orographic cloud over target rises  $2-3^{\circ}\text{C}$  due to pre-band subsidence. CTT  $\sim -25^{\circ}\text{C}$ .
5. Cells weaken near Sierra foothills and trajectories curve cyclonically with southerly 50 kPa winds at Sheridan.
6. Frontal band merges with orographic cloud, CTT rises to near  $-20^{\circ}\text{C}$ .

Period IV: After frontal passage through target area.

1. Orographic precipitation rate remains nearly unchanged following frontal passage. Moist southwesterly flow continues at low levels.
2. CTT of convective orographic cloud  $-10$  to  $-20^{\circ}\text{C}$ .
3. Post-frontal convective bands form along coast parallel to front, organize and grow in the Central Valley, dissipate over Sierra foothills from 1-6 hours after front. Evident in Sheridan precipitation records, not seen in target area precipitation records. CTT  $-30$  to  $-35^{\circ}\text{C}$  in Central Valley.
4. Overlying cirrus deck (if any) clears with passing 30 kPa trough.
5. Convective bands with a secondary cold front may follow 12-15 hours after front passes.

The primary goal of this study was to determine cloud top temperatures over the project area from the satellite infrared data. Comparison of 28 measurements of mean satellite CTT over the target area to cloud truth CTT from soundings, aircraft and radar during the five storms yielded a correlation coefficient of 0.75 between the two sets of measurements. Differences in the measurements are explained mostly by (1) spatial and temporal differences between the measurements, (2) use of the target area average CTT from the satellite and (3) ambiguities in determining cloud tops from the soundings. Better cloud truth comparisons will require careful selection of measurements and will likely have to be done outside the target area. It appears, however, that the satellite is a satisfactory tool for determining cloud top temperatures.

Mean target area CTT for the three storms with cirrus cover and for the three storms without cirrus covering the frontal band was averaged as a function of time from frontal passage at the target (Figure 42). These graphs show that for both cirrus and non-cirrus cases, CTT decreases as the front approaches and is lowest about 1 hour before frontal passage. During and after frontal passage, CTT increases sharply, entering the assumed seeding window range for non-cirrus cases.

Target area CTT is found to be related to the precipitation rate for individual storms. In all cases, low CTT was associated with increased precipitation, although the CTT alone does not yield a precipitation rate that is consistent from one storm to another. On 9 March 1977, when the satellite was definitely viewing the top of the precipitation-producing cloud, a correlation coefficient of 0.76 was found between satellite CTT and the precipitation rate at Blue Canyon. After 0300 GMT on 15 December 1977, multi-layered clouds became a single cloud

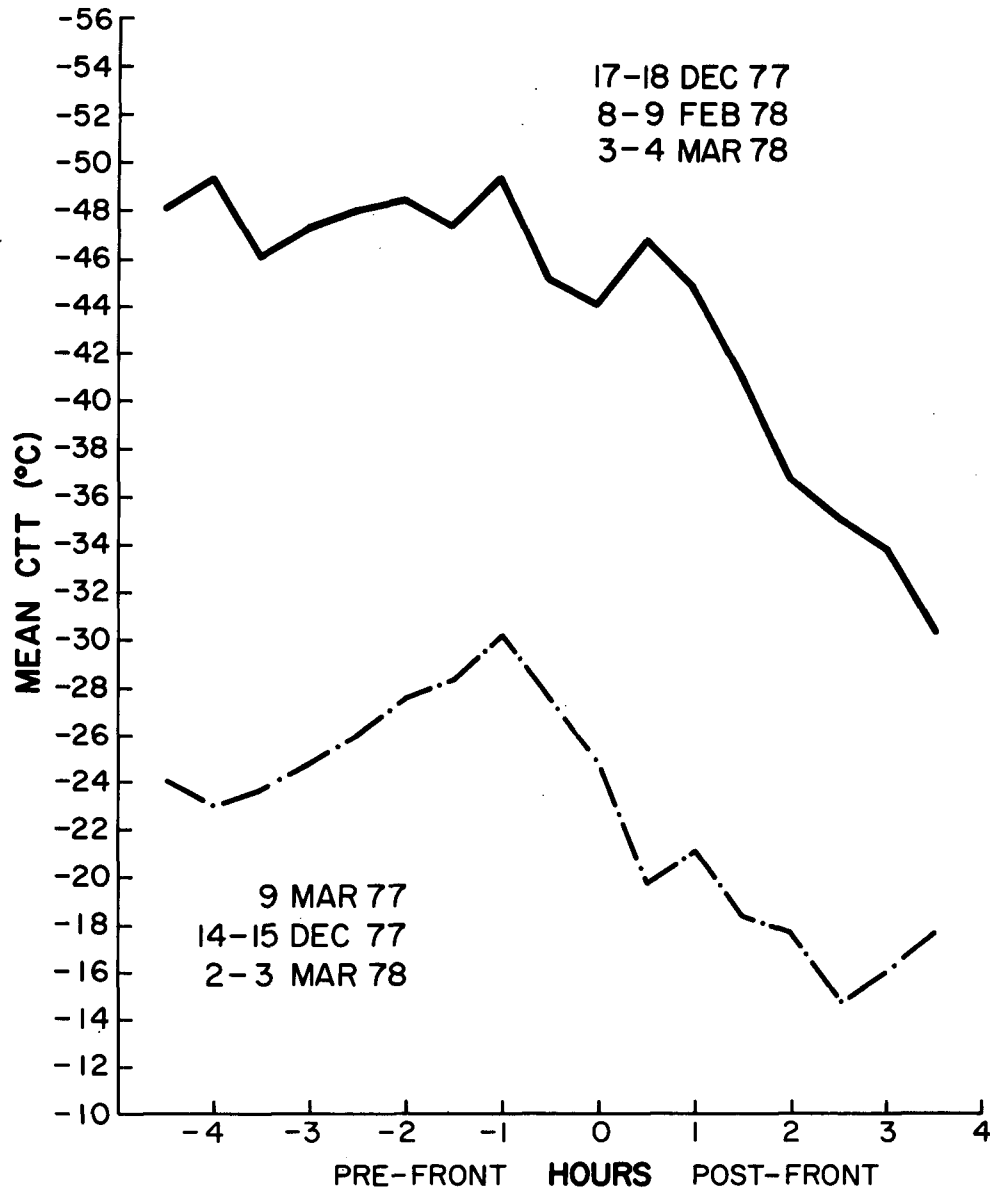


Figure 42. Three storm averages of mean target area CTT relative to time from frontal passage.

layer and a correlation coefficient of 0.82 was found between the above parameters. The precipitation vs. CTT curves for the two days are similar but the 15 December curve gives a higher precipitation rate for the same CTT,

The mean hourly precipitation at Blue Canyon for all six frontal passages vs. time from frontal passage is presented in Figure 43. This graph shows the sudden decrease in precipitation after frontal passage with the highest precipitation rate about 2 hours prior to frontal passage. This curve is nearly identical to the CTT curves shown in Figure 42 and again shows the close relationship of CTT to precipitation.

Precipitation on the lee slopes of the Sierra depends on the presence of cirrus cover on the Sierra orographic cloud. It is not immediately evident whether natural seeding of the orographic cloud by cirrus ice crystals modifies the orographic cloud leading to more precipitation on the lee slopes, or whether the orographic cloud is deeper in these cases, possibly deep enough to form a continuous cloud to the cirrus level. In either situation, precipitation particles would be formed at higher altitudes, and their longer fall time to the surface would allow them to be carried over the Sierra crest and be deposited on the lee slopes. The fact that cirrus does affect precipitation implies that ice crystals are being supplied to the orographic cloud by the cirrus and hence little or no opportunity for precipitation enhancement by artificial cloud seeding exists with cirrus present. It may also have implications for targeting precipitation by artificial seeding, where seeding to imitate the effect of cirrus could produce more precipitation farther downwind. It should be mentioned here that no increase in wind speed at mountaintop levels or above was observed when cirrus cover and

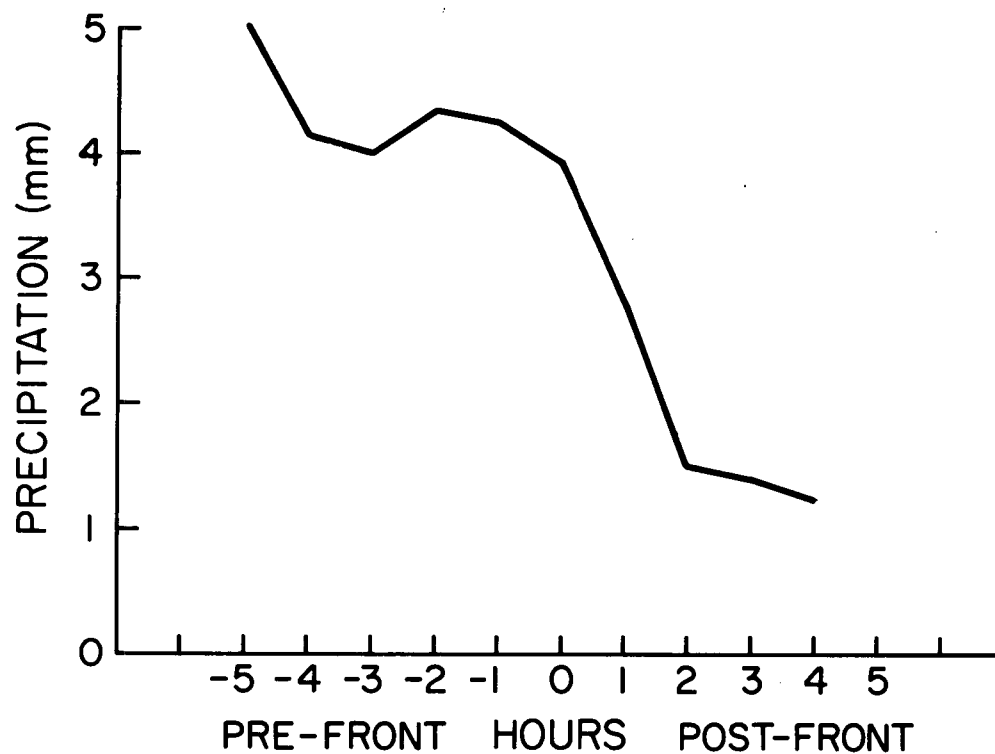


Figure 43. Six storm mean hourly precipitation at Blue Canyon relative to time from frontal passage.

lee precipitation increased. Therefore, a blow-over effect due to high winds did not account for the observed increase in lee precipitation.

The high speed of the cirrus (70 m/s or faster) covering some frontal bands does not hinder the natural seeding process. Cirrus was observed to flow parallel to the frontal band, covering the band along its entire length. With this structure natural seeding by the cirrus could occur despite the high speed of the cirrus, as an ice particle could begin falling far upwind and be able to reach a lower level supercooled water region.

With the exception of the frontal band, convective bands were not observed to be a major feature of Type 1 and 2 storms. Although cirrus obscured the view of the satellite throughout Type 2 storms, no evidence of mesoscale convective bands was present in the target area rain-gage records. Imbedded convection occurs in the orographic cloud following frontal passage, during a period of decreasing precipitation rate. Precipitation from individual imbedded cells was not detectable in half-hourly rain-gage records.

Type 3 storms are dominated by convective bands and large convective cells which generally originate offshore or in the Sacramento Valley. Precipitation in the target area from convective cells accounted for about 25% of the total for the storm, the rest being orographically induced precipitation. Cells that proceeded into the Sierra were observed to dissipate there in most cases.

## 6.0 RECOMMENDATIONS FOR FUTURE WORK

As development of seeding criteria for Sierra cloud systems progresses, it is recommended that the satellite results and speculations presented here be put into perspective with other measurements of seedability, in particular, with aircraft cloud microphysical measurements. The ability of the satellite to determine cloud microstructure from cloud type and cloud top temperature has been assumed at times in this report, but has not often been checked against ground and cloud measurements.

More intensive satellite case studies are needed to determine the reproducibility of the results from the five case studies within this report and lend more credibility to the generalities and definition of three storm types. Also, a larger data base is needed before meaningful climatologies of storms and cloud characteristics can be derived from the satellite viewpoint.

Implementation of the digital satellite in real time to operations of the SCPP at present depends on improved communication between the field project personnel and those involved with the satellite data acquisition and analysis at CSU. Before the real-time potential of digital satellite data can be realized, however, the implications and uses of the satellite digital imagery must be understood by all persons involved. Of course, the best use of digital satellite imagery for SCPP operations will come when the digital data is made available to forecasters and decision makers in the field, which is dependent on the development and procurement of an ADVISAR-type system for project use.

## ACKNOWLEDGEMENTS

This research was sponsored by the U.S. Bureau of Reclamation, Division of Atmospheric Water Resources Management under contract 6-07-DR-20020. Digital satellite data were obtained from the Direct Readout Ground Station (DRGS) of the U.S. Army at White Sands Missile Range, New Mexico. Mr. David A. Matthews of the Bureau of Reclamation was the technical monitor for the contract.

## REFERENCES

- Andrews, M. and R. Fitch, 1979: A digital image system for atmospheric research. CAEE 185, pp. 1-20.
- Brown, M. L., 1978: Digital-video manipulation of satellite imagery. Preprints of Fourth Symposium on Meteorological Observations and Instrumentation, Denver, Colo., pp. 207-211.
- Bureau of Reclamation, 1977: 1976-77 Sierra Cooperative Pilot Project Data Inventory. Denver, Colo.
- Bureau of Reclamation, 1978: 1977-78 Sierra Cooperative Pilot Project Data Inventory. Denver, Colo.
- Elliott, R. D. and E. L. Hovind, 1964: On convection bands within Pacific Coast storms and their relation to storm structure. J. Appl. Meteor., 3, pp. 143-154.
- Grant, L. O., C. F. Chappell and P. W. Mielke, Jr., 1971: The Climax experiment for seeding cold orographic clouds. Preprints of International Conference on Weather Modification, Canberra, Australia, pp. 78-84.
- Grant, L. O., and R. D. Elliott, 1974: The cloud seeding temperature window. J. Appl. Meteor., 13, pp. 335-363.
- Hobbs, P. V., J. D. Locatelli, T. J. Matejka and R. A. Houze, Jr., 1978: Air motions, mesoscale structure and cloud microphysics associated with a cold front. Preprints of Conference on Cloud Physics and Atmospheric Electricity, Issaquah, Wash., pp. 277-283.
- Kreitzberg, C. W. and H. A. Brown, 1970: Mesoscale weather systems within an occlusion. J. Appl. Meteor., 9, pp. 417-432.
- Lamb, D., K. W. Nielsen, H. E. Klieforth and J. Hallett, 1976: Measurement of liquid water content in winter cloud systems over the Sierra Nevada. J. Appl. Meteor., 15, pp. 763-775.
- Marwitz, J. D., 1975: The role of convection for seeding winter orographic storms. Abstracts of Special Regional Weather Modification Conference, San Francisco, Calif., pp. 21-26.
- Marwitz, J. D., R. E. Stewart and J. A. Moore, 1978: Dynamical and microphysical characteristics of winter storms over the Sierra Nevadas. Preprints of Conference of Sierra Nevada Meteorology, South Lake Tahoe, Calif., pp. 1-20.
- Matejka, T. J., R. A. Houze, Jr. and P. V. Hobbs, 1978: Microphysical and dynamical structure of mesoscale cloud features in extratropical cyclones. Preprints of Conference on Cloud Physics and Atmospheric Electricity, Issaquah, Wash., pp. 292-299.

- Peace, R. L., 1975: Radar observations of Sierra snowstorms. Abstracts of Special Regional Weather Modification Conference, San Francisco, Calif., pp. 125-130.
- Reynolds, D. W., 1977: Satellite studies during the 1976-1977 Sierra Cooperative Program. Annual Report to the Bureau of Reclamation, Contract No. 6-07-DR-20020, Denver, Colo., 43 pp.
- Reynolds, D. W. and K. R. Morris, 1978a: Use of the ADVISAR in the analysis of digital satellite data for operational seed-no seed decision making. Preprints of Fourth Symposium on Meteorological Observations and Instrumentation, Denver, Colo., pp. 212-218.
- Reynolds, D. W. and K. R. Morris, 1978b: Satellite support to the Sierra Cooperative Pilot Project. Preprints of Conference on Sierra Nevada Meteorology, South Lake Tahoe, Calif., pp. 141-148.
- Smith, E. A. and D. R. Phillips, 1972: Automated cloud tracking using precisely aligned digital ATS pictures. IEEE Transactions on Computers, C-31,7,715-29.
- Sutherland, J. L., C. Wisner and D. E. Hughes, 1977: Sierra Cooperative Pilot Project - a radar climatology of Sierra Nevada winter storms. Interim report to Bureau of Reclamation, Contract No. 6-07-DR-20130, Denver, Colo., 134 pp.

<b>BIBLIOGRAPHIC DATA SHEET</b>		1. Report No.	2.	3. Recipient's Accession No.	
4. Title and Subtitle				5. Report Date	
Satellite Studies During the 1976-77 1977-78 Sierra Cooperative Pilot Project				February, 1979	
7. Author(s)				8. Performing Organization Rept. No.	
K. R. Morris, D. W. Reynolds and T. H. Vonder Haar					
9. Performing Organization Name and Address				10. Project/Task/Work Unit No.	
Atmospheric Science Department Colorado State University Fort Collins, CO 80523				11. Contract/Grant No. 6-07-DR-20020	
12. Sponsoring Organization Name and Address				13. Type of Report & Period Covered	
Office of Atmospheric Resources Management Bureau of Reclamation Denver Federal Center Denver, CO 80225				Final Report	
				14. 2 Dec 75 to 30 Sept 78	
15. Supplementary Notes					
16. Abstracts					
<p>Digital satellite data from the SMS-2 geostationary satellite have been analyzed for the 1976-77 and 1977-78 seasons of the Sierra Cooperative Pilot Project. Temporal variations in cloud top temperature (CTT) and mesoscale and synoptic cloud features for five case study storms are presented. Highest precipitation rate and lowest cloud top temperature were found to occur 1-2 hours before surface cold frontal passage during the merger of the frontal cloud band with the Sierra orographic cloud. CTT was near <math>-35^{\circ}\text{C}</math> and below the lower seeding threshold at this time. An unstable convective orographic cloud remained over the Sierra for up to 8 hours after frontal passage with CTT near <math>-15^{\circ}\text{C}</math>.</p> <p>Three storm types and associated synoptic conditions have been defined by the satellite viewed cloud types. Mesoscale features and their precipitation effects have been observed.</p>					
17. Key Words and Document Analysis.			17a. Descriptors		
Digital Satellite Imagery Weather Modification Cloud Top Temperature Sierra Nevada Storm Cloud Types Precipitation Effects			Abstract continued  Convective cells were tracked onshore and the effects of the Sierra on the cells were studied. Precipitation on the lee side of the Sierra was found to depend on the presence of high, cold clouds.		
17b. Identifiers/Open-Ended Terms					
17c. COSATI Field/Group					
18. Availability Statement			19. Security Class (This Report)		21. No. of Pages
			UNCLASSIFIED		89
			20. Security Class (This Page)		22. Price
			UNCLASSIFIED		